A SCREW THEORY APPROACH TO ANALYZE THE DYNAMICS OF PARTS IN A VIBRATORY BOWL FEEDER

by

Julio César Castro Aguila

A thesis submitted in partial fulfillment of the requirements for the degree of

MASTER OF SCIENCE
in
MECHANICAL ENGINEERING

UNIVERSITY OF PUERTO RICO
MAYAGÜEZ CAMPUS
2008

Approved by:

David Dooner, Ph.D. Member, Graduate Committee	Date
David Serrano, Sc.D. Member, Graduate Committee	Date
Lourdes M. Rosario, Ph.D. President, Graduate Committee	Date
Cristina Pomales García, Ph.D. Representative of Graduate Studies	Date
Paul A. Sundaram, Ph.D. Chairperson of the Department	Date

Abstract

Vibratory bowl feeders are widely used in automatic assembly lines. The availability of good models to predict the behavior of parts inside of them is highly useful.

This work presents a method that predicts the natural resting aspects probability profile for three parts named “T” shape, Arc Chute and Magnet under a new approach based on its inertial properties. The work also analyzes the dynamic behavior of the parts Arc Chute and Magnet on a vibratory bowl feeder. The analysis studied the part’s behavior on the bowl floor and bowl track. The main parameters governing the transport phenomena were modeled for values used in analysis made by previous researchers.

In general, the probability profile is directly proportional to the mass distribution around an axis perpendicular to the plane of the resting aspect (coincident with the center of gravity), and inversely proportional to the height of the center of gravity. This represents an advantage over previous methods, due to simplicity, easy implementation and visualization for parts with complex geometries.

RESUMEN

Los alimentadores vibratorios son ampliamente usados en líneas de ensamblaje automatizadas. La disponibilidad de buenos modelos que predigan el comportamiento de piezas en su interior es altamente útil.

Este trabajo presenta un método que predice la probabilidad de descanso natural de tres piezas llamadas forma “T”, Arc Chute y Magnet bajo un nuevo enfoque basado en sus propiedades inerciales. El trabajo también analiza el comportamiento dinámico de piezas Arc Chute y Magnet al interior de un alimentador vibratorio. El análisis estudia la conducta de las piezas en el piso del tazón del alimentador y en el carril inclinado del alimentador. Los parámetros principales que gobiernan el fenómeno de transporte fueron modelados para valores usados en trabajos realizados por investigadores previos.

En general, el perfil de probabilidades es directamente proporcional a la distribución de masa alrededor de un eje, perpendicular al plano del aspecto de descanso y coincidente con el centro de gravedad, e inversamente proporcional a la altura del centro de gravedad medida desde ese aspecto. Esto representa una ventaja considerable con respecto a otros métodos usados, debido a la simplicidad, fácil implementación y visualización para partes con geometrías complejas.

To: mi Dios, papá y mamá

ACKNOWLEDGEMENTS

During the development of my graduate studies in the University of Puerto Rico, several persons and the institution collaborated directly and indirectly with my research. Without their support it would be impossible for me to finish my work. That is why I wish to dedicate this section to recognize their support.

I want to start expressing a sincere acknowledgement to my advisor, Dr. Lourdes Rosario because she gave me the opportunity to research under her guidance and supervision. I received motivation; encouragement and support from her during all my studies. With her, I have learned about writing technical documents and sharing my ideas with the public. I also want to thank the example and support I received from Dr. David Dooner. From these two persons, I am completely grateful. Special thanks I owe Dr. Paul Sundaram for his constant attention to my studies. I would like to thank the Mechanical Engineering Department, University of Puerto Rico Mayagüez Campus for giving me the opportunity to work in my master degree.

At last, but the most important I would like to thank my family, for their unconditional support, attention and love.

TABLE OF CONTENTS

LIST OF TABLES

Tables **Page**

LIST OF FIGURES

Figures **Page**

NOMENCLATURE

A_0: Vibration amplitude.

Ai: Contact area of the aspect i

CSA: Centroid solid angle.

F_N: Normal force between two surfaces.

g: Gravity acceleration.

Hi: Height of the Centroid from aspect i.

Ii: Polar moment of inertia from aspect i.

$[I_C]$: Inertia matrix at the center of gravity, measured in the directions of the body frame.

MDBT: Modified dynamic bowl test.

MDFT : Modified dynamic feeding test.

Pi: Probability of the natural resting aspects in aspect i.

PMI: Proposed method to compute resting aspects probability profile

Qi: Centroid solid angle subtended by aspect i.

R_1 : Reaction of the bowl wall.

R_{1f} : Friction force due to reaction R_1.

R_2: Reaction of the bowl wall.

R_{2f} : Friction force due to reaction R_1.

R_3 : Friction force in the direction of Y´.

R_4: Friction force in the direction of X´.

R_y : Friction force in direction Y.

R_z : Friction force in direction Z.

V_X: Velocity in the x direction.

V_Y: Velocity in the y direction.

V_Z: Velocity in z direction.

X: Fixed axis.

X´: Mobile axis fixed to part at c.

Y: Fixed axis.

Y´: Mobile axis fixed to part at c.

Z: Fixed axis.

Z´: Mobile axis fixed to part at c.

GREEK SYMBOLS

α: Excitation angle respect to x axis.

β: Excitation angle respect to xy plane.

ε: Dual number.

δ: Inclination angle of the track around x axis.

γ: Inclination angle of the track around y axis.

μ_k: Kinetic friction coefficient.

θ: Rotation angle about x axis.

σ: Application angle of the normal force between the part and the bowl wall.

ω: Angular frequency of vibration.

1 INTRODUCTION

The vibratory bowl feeder is a widely used device in automated manufacture to sort, orient and deploy parts in preferred directions to automated workheads or robots.

The design of a feeder is based on the part's features and process requirements. Some features of interest are: size, shape, preferred orientation and roughness. The important process requirements are volume and production rate. These requirements are defined by the manufacturer. The feeder design process begins by determining the most probable resting aspects for the parts to be oriented and finding the part's probability profile. The part´s probability profile is the probability distribution of the natural resting faces and orientation of the parts. The bowl and tracks are dimensioned according to the part´s size. Then the designer selects the orienting device to be used, and tests are performed in a basic feeder to optimize the performance of the feeder. (Rincón, 2002).

The study of natural resting aspects and spatial motion of parts inside a bowl feeder provides good information to improve the feeder efficiency (the ratio of the number of parts properly fed to the workhead to the number entering the system, (Ngoi, 1995) and the orientation mechanisms. Previous researchers have been working with the natural resting probability profiles for regular parts and some complex parts. Various approaches have been used as Centroid Solid Angle CSA, stability method, displaced center of gravity method and dynamic drop tests (Boothroyd, 1992, Ngoi, et al. 1995 a-d). Screw Theory has been developed for over 100 years. It is well known to describe a set of forces and velocities acting on a rigid body. According to this, it will be used to describe the kinetic and kinematic relationships between the parts and the vibratory bowl feeder.

1.1 PROBLEM DESCRIPTION

The Screw Theory has been used to describe the behavior of solids in the space, and applied to automatic robots handling. To our knowledge, no articles in the literature known uses it to analyze complex geometry parts inside a vibratory bowl feeder. This research consists on the evaluation of a method to compute the resting aspects probability profile and the development of equations, based on the Screw Theory, to analyze the dynamic behavior of two parts, previously tested in the work of Santos, 2004. The study of dynamic behavior will include the influence of bowl track parameters as well as parts parameters. Bowl track parameters will be amplitude and frequency of vibration, angle of inclination and friction coefficient. Parts parameters will be geometry, inertia and a set of forces acting or reacting on them. The mathematical analysis and equations based on this theory will simulate the transport process of the parts in the bowl base and disclose the governing equations through the bowl track.

1.2 OBJECTIVES

This research is aimed to apply the Screw Theory to analyze the static and dynamic behavior of specific parts inside a vibratory bowl feeder. The results will then be compared to experimental data obtained by previous researcher. (Santos, 2004, and Ngoi, 1995).

The research objectives are:

1. Propose a Hypothesis to evaluate the natural resting aspect probability profile of complex parts: "T" shape, Arc Chute and Magnet.
2. Apply the Screw Theory to study the dynamic behavior of two selected parts Arc Chute and Magnet that were studied in Santos's work, (Santos, 2004). The analysis will be performed for horizontal floor and inclined track.
3. Plot surface graphics of the analysis results of the part Arc Chute on the bowl floor. Typical parameter will be assumed as related by Boothroyd, 1992, and Diaz, 2004.
4. Compare the deviations between the dynamic probability and static probability profiles obtained for the parts using the station developed by Rincón (Rincón, 2002), with the results given by the proposed method.
5. Draw conclusions and future work guidelines.

Originally, the objectives included measuring the part's transport velocity and acceleration. However, it was not possible to measure these parameters due to the lack of appropriate instrumentation. Instead of that, the results for the probability profiles where compared with available analytical and experimental data for parts.

1.3 PROCEDURE

The research methodology consists of a reviewing the Screw Theory formulation and application of relevant topics to selected parts. These steps will be described next.

1) Perform a revision of the Screw Theory in order to get the relevant mathematical formulation describing the physical kinematic phenomenon of a solid in general spatial motion.
2) For the parts named "T" shape, Arc Chute and Magnet:
   a) Analyze the resting aspects probability profile trough a proposed hypothesis.
   b) Compare the results with data obtained from previous researchers: Santos, 2004; Ngoi et al. 1995.
3) For the parts named Arc Chute and Magnet:
   a) Study their dynamic behavior with the Screw Theory based on the Screw Theory formulations. Figures 1-1 and 1-2 show these parts.
      i) To perform this analysis, the first step will be to reduce a set of external forces acting on the part to a wrench, a force screw and an angular momentum screw, based on the Poinsot Theorem.

ii) Two reference frames will be used for both parts, one attached to the centre of mass of the part or body frame and another one fixed on the motion plane of the part (the base) or the inertial frame. Then, the boundary conditions will be applied to those screws in order to determine the limiting condition for part motion.

iii) The analysis will be performed on the bowl base and then on the narrow track, taking into account the track reactions for the wall caused by the track angle and bowl radius.

b) Predict the influence of selected parameters in the transport process of the selected parts through the bowl base. These parameters will be: frequency of vibrations, amplitude of vibration and friction coefficient.

4) Draw conclusions.

The “T” shape part was added to the analysis due to its facility for studying a family of parts, varying the aspect ratio, and the considerable amount of available experimental data by previous researchers

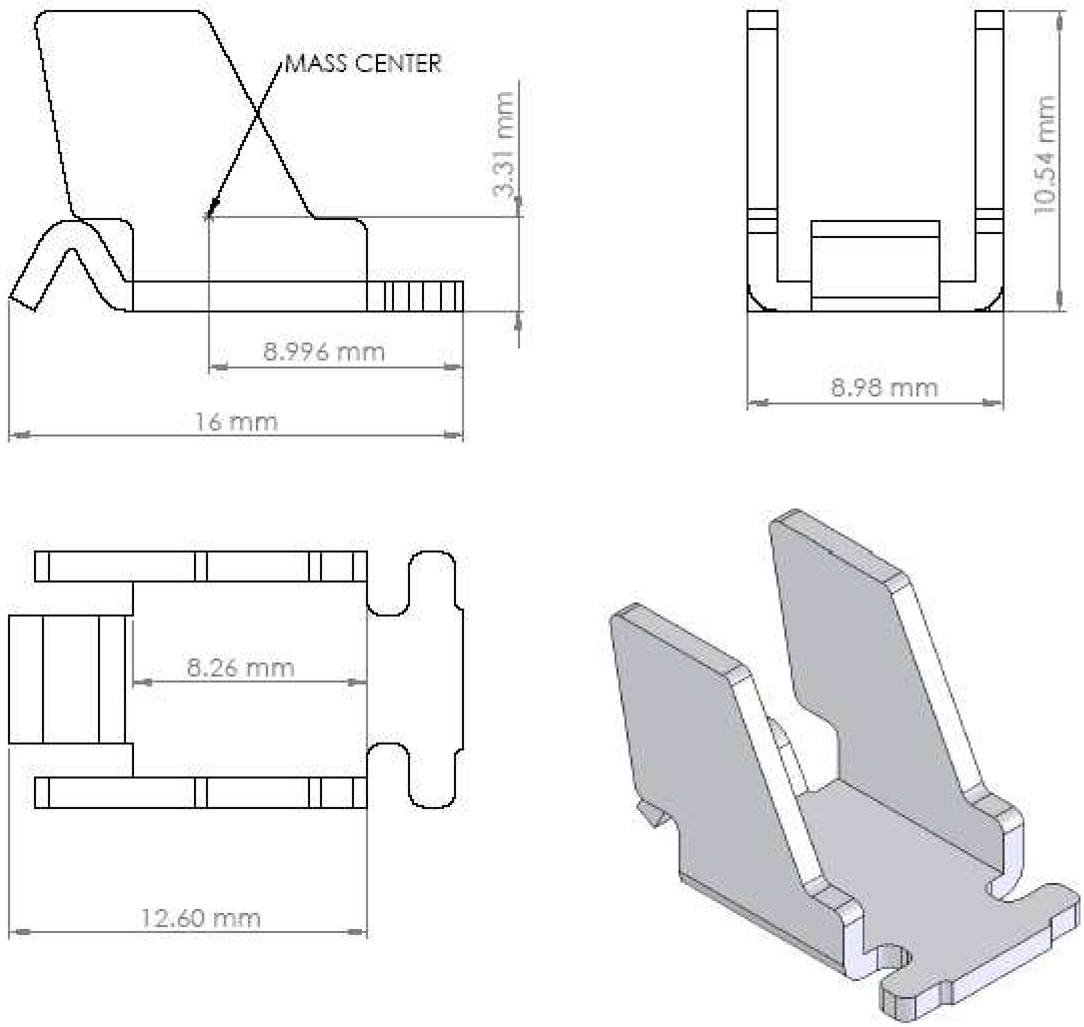

Figure 1-1. Arc Chute views and dimensions

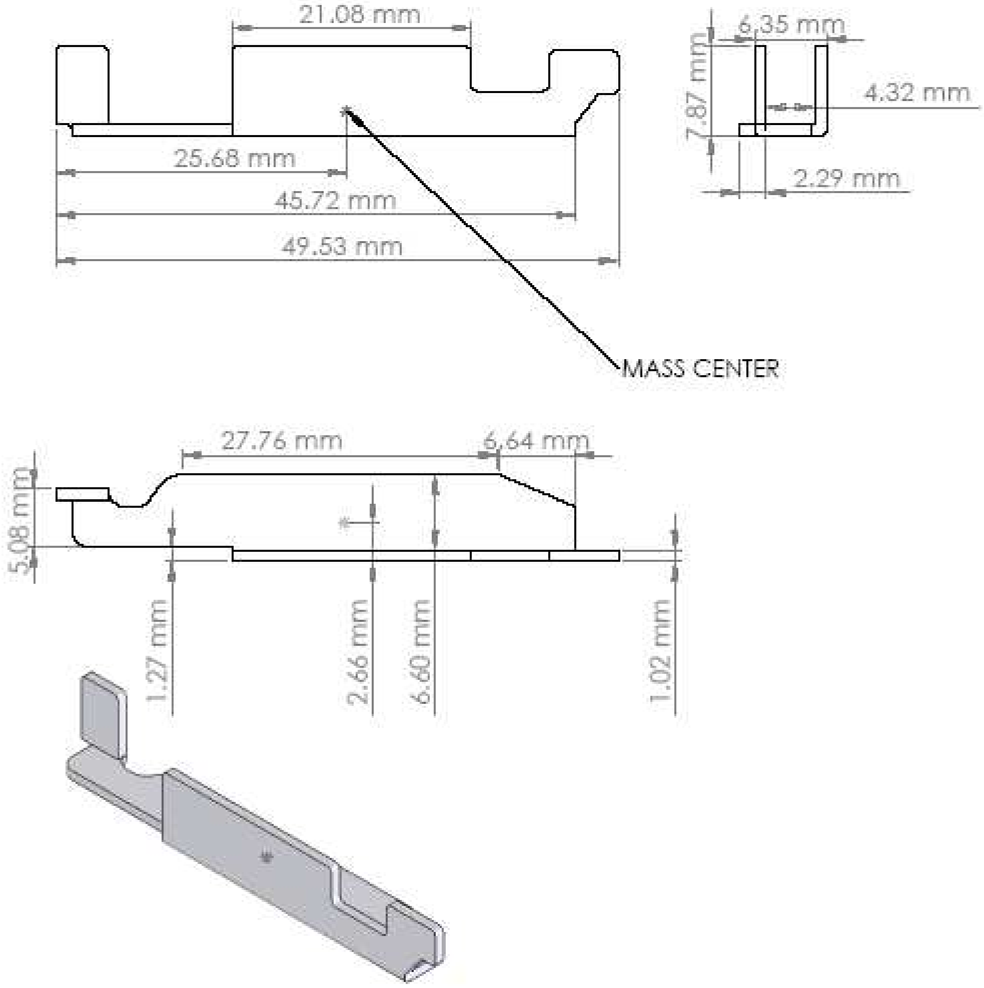

Figure 1-2. Magnet views and dimensions

1.4 SUMMARY

In this chapter the importance of the analysis of parts inside vibratory bowl feeders was discussed. It provides good information that lead to more precise control of the orientations of the parts, as they leave the bowl, improving the feeder efficiency, and the orientation mechanisms. Three parts will be used for the study of natural resting aspects: "T" shape, Arc Chute and Magnet. The "T" shape was included due to its facility to study a family of parts varying the aspect ratio and the amount of available experimental data by previous researchers for this type of part. The dynamic analysis was performed for the parts Arc Chute and Magnet.

The main parameters accounted for designers in order to improve the feeder's efficiency were presented. The efficiency referred to the ratio of the number of parts properly fed to the workhead to the number entering the system, Ngoi, 1995). This chapter also described the main objectives of this research, regarding the use of Screw Theory to analyze the static and dynamic behavior of selected parts, and how these objectives will be developed.

The next chapter presents a discussion regarding screws, systems of coordinates and formulas from Screw Theory. The third chapter presents the analysis of natural resting aspects for complex parts. The fourth chapter presents the study of parts arc chute and magnet applying the principles discussed in Chapter 2. The fifth chapter presents graphics of the main parameters governing the transport phenomena of the part Arc Chute. The last chapter discuss about the main conclusions derived from the work and future guidelines to continue in this line of research.

2 LITERATURE REVIEW

The kinematic, static and dynamic properties of a rigid body are fundamentally screws; therefore the Screw Theory is convenient to describe a system of forces, displacements and velocities, as well as other entities which form a helicoidal field. This theory has been applied to the dynamic analysis of a rigid body in general spatial motion, placing emphasis on the geometrical interpretation of those entities. The dynamic state of motion of the body is then described by a dual vector equation, referred as the dual Euler equation with a geometric equivalent as a spatial triangle of screws. (Pennock and Oncu, 1992).

Several researchers worked with theoretical and practical methods to predict the probability profiles of the parts to be oriented. Other researchers have successfully applied kinematic formulations to validate those methods using the multibody theory, friction and collision of parts. (Díaz, 2004 and Rincón, 2002).

Díaz applied the multibody theory in the analysis of the behavior of interconnected parts colliding inside a vibratory bowl feeder. The analysis was based on the dynamic behavior of impact as it affects the parts natural resting aspects. He studied the collisions of interconnected cylindrical parts, the collisions of parts and bowl track and the collision of parts and bowl wall. He also applied the Screw Theory to describe the dynamic behavior of cylindrical parts on the horizontal plane, evaluating the friction forces on the case of rolling motion for the cylinder. The

Coulomb friction equation is the linear relationship between the normal force and the friction force. This equation is correct for the maximum static and kinetic forces. In the case of rolling motion of the cylinder, the friction forces are not necessary maxima, so the friction force must be found to complete the dynamic analysis (Díaz, 2004).

The geometric relationship between velocity screws and momentum screws were used to define the called centripetal screw, by means of the dual angle formed by them. The centripetal screw proved to be a useful tool in the study of the dynamics of a rigid body. Besides, the dual Euler equation which is the dual form of the Newton-Euler equation of motion is shown to be a spatial triangle as shown in Figure 2-1. The vertices of the triangle are the centripetal screw, the time rate of change of the momentum screw and the force screw. The sides of the triangle are three dual angles between the vertices. The spatial triangle provides valuable geometrical insight into the dynamic of a rigid body. (Pennock and Meehan, 2002).

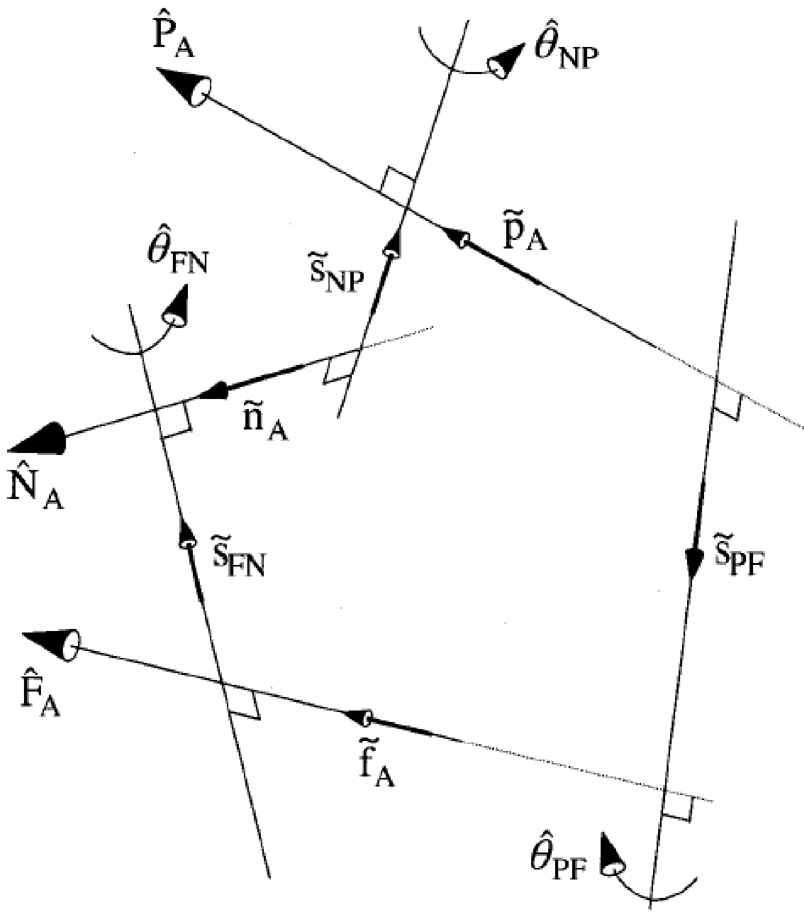

Figure 2-1. Spatial triangle formed by three screws as sides (Pennock, 2002).

Where: $\hat{n}_A$ is the time rate of change of momentum screw

$\hat{f}_A$ is the force screw

$\hat{p}_A$ is the cross product screw of velocity screw and angular momentum screw.

Based on the screw triangle it has been shown that Screw Theory is very susceptible to easy geometric interpretation. This geometric interpretation makes the theory a useful tool to the kinematics, kinetics and dynamic force analysis of spatial robot manipulators. (Pennock, 1992). As an example Wang, using the definition of pitch by Dimentberg, demonstrated that all possible screws for the finite displacement of bodies form a screw system of the third order. In this approach the spatial screw triangle defined by Pennock and Meehan, 2002, and analytical geometry are used to demonstrate the formation of the system. (Wang and Huang, 2003).

2.1 THE THEORY

Sir Robert Stawell Ball defined the screw as: “a screw is a straight line with which a definite magnitude termed the pitch is associated” (Ball, 1900). The line is referred as the axis of the screw, the pitch is the ratio of translation to rotation along the axis and a scalar magnitude, named the amplitude of the screw, is the amount of rotation about that axis.

Screw Theory is based on two fundamental theorems:

1. Chasles theorem: Rigid body motion is equivalent to twist on a screw, rotation about a unique axis and translation parallel to the axis. (Lipkin and Duffy 2002).
2. Poinsot theorem: Rigid body action is equivalent to a wrench on a screw, force along a unique line and a couple parallel to the line. (Lipkin and Duffy 2002).

Particular or special cases are screws with infinite pitch, called infinite screws and screws with zero pitch. Infinite pitch screws correspond to free vectors in which the pitch becomes indeterminate because no angular quantity exists and only the linear component is present. This causes the line to become a vector carrying a scalar magnitude. Screws with zero pitch are called line vectors because they are pure rotational, since points along the axis have pure rotation, causing the pitch to become zero.

2.2 NOTATION FOR SCREWS

Several ways are in use to describe screws. The most common are: vector representation, dual numbers, Plucker coordinates and Lie Algebra.

In Vector representation, a screw is presented as two classical vectors, one the angular quantity vector and another one, the total effect vector, which includes the total velocity and the total force.

$$(\omega, v_p) = (\omega, r_p \times \omega + h\omega)$$
$$(f, m_p) = (f, r_p \times f + hf)$$

Where: **r** represents a vector directed from point to the screw
f and **m** the resultant force and moment vector
w and **v** were respectively the resultant angular and linear velocity vector, all of them referred to **p**.
h represents the pitch.

In Dual numbers, the screw is represented by the use of the operator ε, knowing that the $\varepsilon^2 = 0$ equality must always be satisfied. This is analogous to the imaginary operator i, where $i^2 = -1$. Where the first term is the scalar and the second one, accompanied by the ε, is called the dual number.

$$\omega + \varepsilon v_p = (\omega + \varepsilon h\omega)(s + \varepsilon r_p \times s)$$
$$f + \varepsilon m_p = (f + \varepsilon hf)(s + \varepsilon r_p \times s)$$

The Plucker coordinates notation, is the most versatile and used notation of all, because those are well related to vector algebra and spatial geometry nomenclature. In this notation the screws are denoted by their homogeneous coordinates and cross product between the ray coordinates of the line and the vector position of **r** Davidson and Hunt, 2003.

$$\begin{bmatrix} v_o \\ \omega \end{bmatrix} = \omega \begin{bmatrix} r_o \times s + hs \\ s \end{bmatrix}$$
$$\begin{bmatrix} f \\ m_o \end{bmatrix} = f \begin{bmatrix} s \\ r_o \times s + hs \end{bmatrix}$$

Where **w**, **v**, **f** and m have the same meaning as before and $\mathbf{r_o}$ is the vector position of **r** from the origin and **s** is the unit line vector.

The basic operation, properties and definitions for screws are: screw definition, arithmetic operations, screw dot product, screw cross product, momentum and velocity screw. These operations will be described next. (Davidson and Hunt, 2003; Lipkin and Duffy, 2002).

Defining the screws:

$$\hat{S}_A = (a + \varepsilon b)$$
$$\hat{S}_B = (c + \varepsilon d)$$

The arithmetic operations are:

$$(a + \varepsilon b) \pm (c + \varepsilon d) = (a \pm c) + \varepsilon (b \pm d)$$
$$(a + \varepsilon b)(c + \varepsilon d) = (ac) + \varepsilon (ad \pm bc)$$
$$(a + \varepsilon b) / (c + \varepsilon d) = [(ac) + \varepsilon (ad - bc)] / c^2$$

The cross product operator between screws $\hat{S}_1$ and $\hat{S}_2$ is:

$$\hat{S}_1 \otimes \hat{S}_2 = (S_1 + \varepsilon S_{10}) \otimes (S_2 + \varepsilon S_{20}) = S_1 \times S_2 + \varepsilon (S_1 \times S_{20} - S_2 \times S_{10})$$

The screw velocity is defined as the screw formed by the angular velocity and the linear velocity:

$$\hat{S}_{\hat{V}_a} = (\vec{\omega}; \vec{V}_a) = \vec{\omega} + \varepsilon \vec{V}_a \qquad [2.1]$$

The Linear momentum vector of mass center for a rigid body is defined as the scalar product of body mass and the vector formed by the linear velocity and the cross product of angular velocity and the vector position from the mass centre:

$$\vec{q} = m(\vec{V}_a + \vec{\omega} \times \vec{A}\vec{G}) \qquad [2.2]$$

with $\vec{A}\vec{G}$ as position vector from point **A** to mass center **G**

Angular momentum vector of mass center for a rigid body is defined as the sum of the vector formed by the angular velocity plus the body inertia matrix and the scalar product of body mass and the vector formed by the cross product of vector position from the mass center and the linear velocity:

$$\vec{H}_a = [I_a]\varpi + m\left(\vec{A}\vec{G} \times \vec{V}_a\right) \qquad [2.3]$$

The momentum screw is defined as the screw formed by linear momentum vector of mass and angular momentum vector of mass:

$$\hat{S}_{\vec{H}_a} = \left(\vec{q}; \vec{H}_a\right) = \vec{q} + \varepsilon \vec{H}_a \qquad [2.4]$$

2.3 SUMMARY

The study of the spatial motion of parts inside a bowl feeder provides good information to improve feeders efficiency, the ratio of the number of parts properly fed to the workhead to the number entering the system (Ngoi, 1995), and the orientation mechanism. This chapter explained the basic ideas concerning Screw Theory, which has been developed for over 100 years; it is well known to describe a set of forces and velocities acting on a rigid body and so can describe the kinetic and kinematic relationships between the parts and the bowl inside a vibratory bowl feeder. The fourth chapter will describe this relationship for two parts, named Arc chute and Magnet. Based on this, a model of the transportation dynamic phenomenon will be derived.

3 ANALYSIS OF THE NATURAL RESTING ASPECTS OF PARTS: "T" SHAPE, MAGNET AND ARC CHUTE

"If a quiescent rigid body has freedom of the n order, then n screws can always be found, such that if the body receives an impulsive wrench on any one of the screws, the body will commence to twist about the same screw"

(Ball, 1900)

This chapter presents the analysis of the natural resting aspects of a "T" shape test part as shown in Figure 3-1, and the part named magnet and arc chute previously analyzed by Santos. Natural resting aspects are defined as the preferred orientations that a given part takes when dropped on a surface, in this case a vibratory bowl feeder. A good vibratory bowl feeding system transports parts in their natural resting aspects with the highest probability values, using a minimum number of orienting devices. Consequently, the efficiency, or the ratio of the parts properly fed to the number of parts entering the feeding system, will be high (Lee, Lim and Ngoi, 1996).

This chapter presents a new approach in the analysis of natural resting behavior of a part with complex geometry. Previous researchers have worked with geometrical methods as Centroid Solid Angle (CSA), Stability method, Energy Barrier method and Dynamic Tests, to find the probability profile of the various aspects of regular parts. Complex parts were analyzed with the aid of some modifications to the original geometry (i.e. virtual faces, solid volumes, empirical factors).

The hypothesis presented here is that there is a direct correlation between some part's geometric feature when it lays in certain orientation and the probability of the natural resting aspects of the part in that same position. A possible feature is the polar moment of inertia. The polar moment of inertia is a measure of the mass distribution around an axis. The probability of a part to rest on a particular aspect is proportional to the value of the polar moment of inertia for the inertia screw perpendicular to the aspect analyzed (coincident with the center of gravity). The probability is inversely proportional to the height of the centre of gravity. The product of the polar moment of inertia divided by the height of the center of gravity for a given aspect will be called PMI for simplicity. To test the hypothesis three parts will be analyzed: A sample symmetrical "T" shape part, the part arc chute and magnet. The results will be compared with results obtained by previous researchers.

The method takes the assumption that the surfaces can be classified as hard and soft, (Boothroyd, 1992). When a part falls on a hard surface, the impact force has a significant vertical component, which imparts a wrench to the part, which in turn causes the part to roll over, changing from one aspect to another. During this process, the part tends to rest on an aspect with the largest contact area, in an attempt to transmit as much of its internal energy to the surface as possible. On the other hand, this change must overcome the stability given by the mass distribution around the axis perpendicular to the resting aspect plane. The inertia values will be computed using a model created in the design software Solid Works and the tool: "physic properties of the solid".

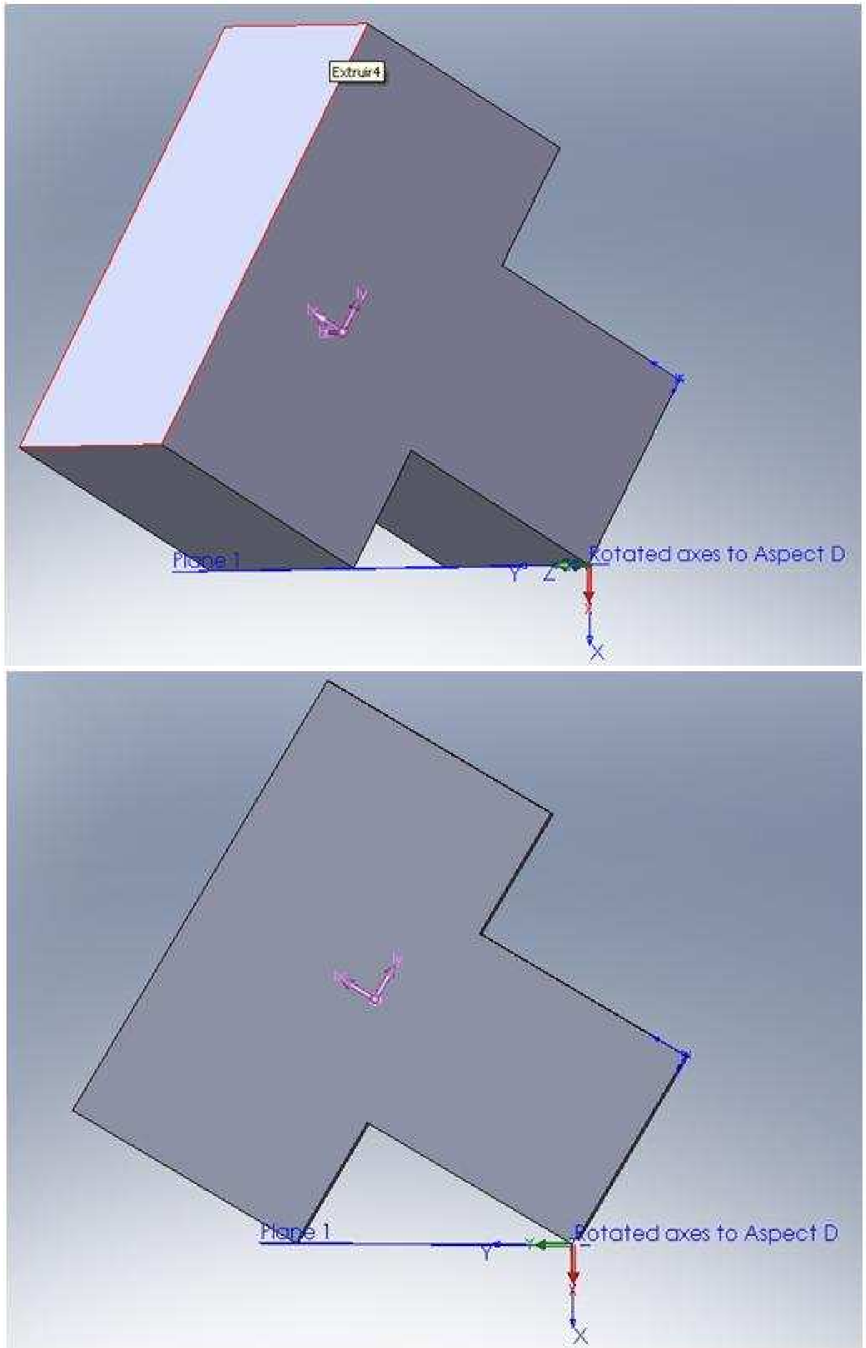

Figure 3-1. Inertia axes orientation for "T" part in Solid Works.

Figure 3-2 shows the natural resting aspects of this shape. This part has five possible resting aspects. The first four aspects are referred to the "T" shape sides. Aspect E is when the part lies flat on the surface.

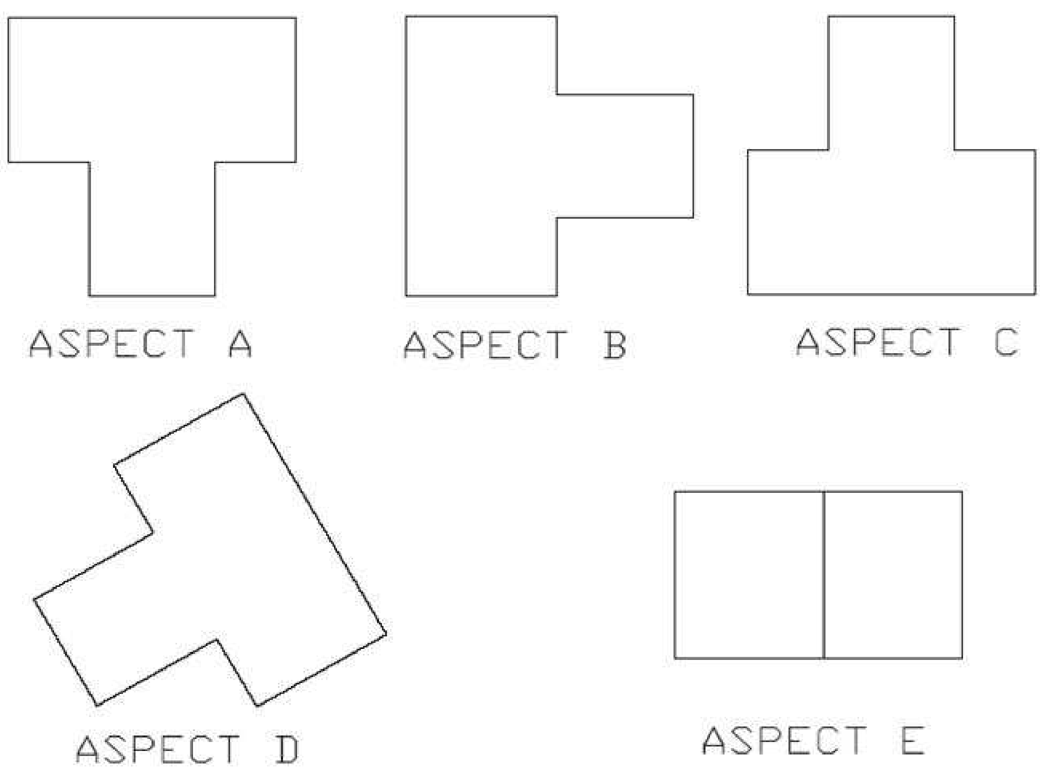

Figure 3-2. Natural resting aspects of "T" shape

Figure 3-3 shows the dimensions of a T-shape part. Table 3-1 provides a summary of the results of the probabilities for each natural resting aspect of this part. These results are based on the work described by Ngoi (1995-d).

Figure 3-4 shows the possible aspects of part Arc Chute. Tables 3-2 through 3-4 summarize the results of the parameters calculated and probabilities obtained by Santos for these aspects (Santos, 2004).

Table 3-1
Probability distribution: CSA method and experimental data for part "T". Aspect Ratio of 0.6 (Ngoi 1995-d).

Aspect	Probabilities CSA method	Probabilities Experimental Data
A	1	0.4
B	6	1.8
C	7	9.74
D	5.60	9.2
E	80.4	78.74
Total	100.00	100.00

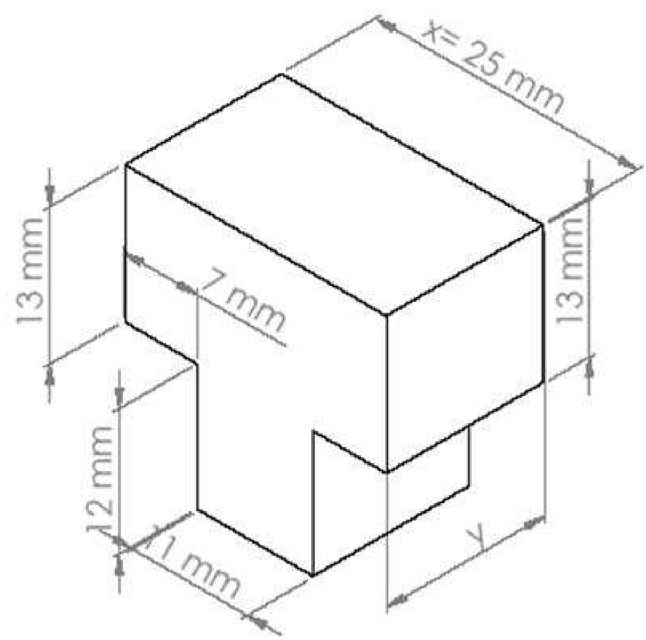

Figure 3-3. Dimensions of "T" shape.

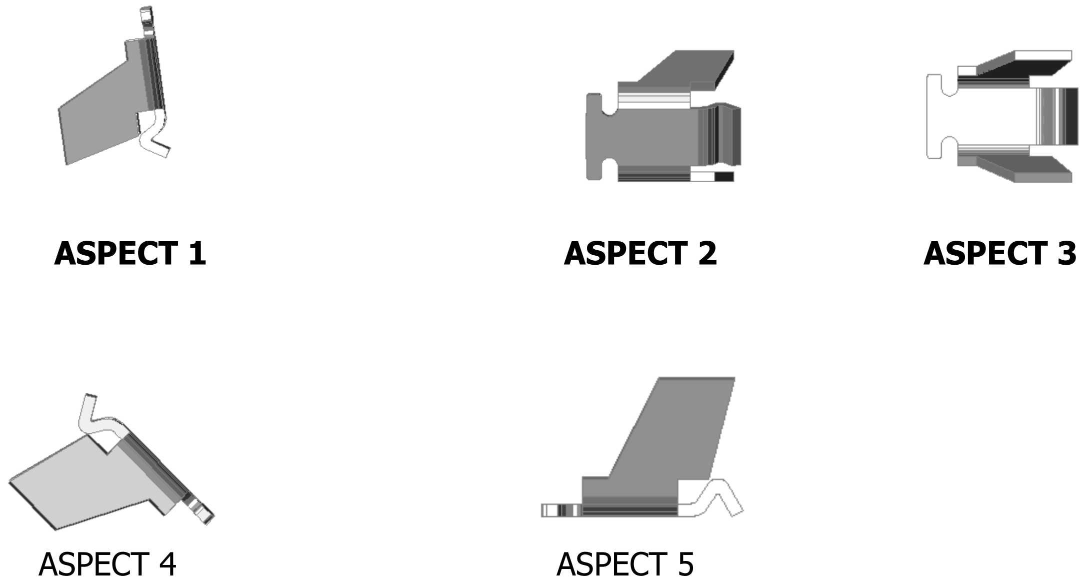

Figure 3-4. Natural resting aspects of part Arc Chute (Santos, 2004).

Table 3-2. Probability distribution: CSA method for part Arc Chute (Santos, 2004).

Aspect	Qi	hi	Htotal/hi	Qi/hi	Probability
1	18.0756	10.1419	1.113144	1.78227	0.08134
2	29.8701	7.4007	1.52545	4.03612	0.18421
3	29.8703	7.4007	1.52545	4.03615	0.18421
4	36.3687	7.4007	1.52545	4.91422	0.22429
5	37.2037	5.2094	2.167121	7.14165	0.32595
Total	133.313			21.9104	1

Table 3-3.Probability distribution: stability method for Arc Chute (Santos, 2004).

Position	Ai	Hi	Ai / Hi	Probability
1	100.321	10.1419	9.8917	0.15211
2	46.3172	7.4007	6.25849	0.09624
3	46.3172	7.4007	6.25849	0.09624
4	158.885	7.4007	21.469	0.33014
5	110.186	5.2094	21.1514	0.32526
Total	462.027		65.029	1

Table 3-4
Experimental Data for different vibration amplitudes per Arc Chute (Santos, 2004).

Aspect	MDBT			MDFT		
	78%	80%	82%	78%	80%	82%
1	0.022	0.012	0.018	0.013	0.009	0.008
2	0.343	0.035	0.032	0.059	0.07	0.074
3	0.209	0.049	0.031	0.082	0.083	0.08
4	0.177	0.278	0.295	0.281	0.273	0.26
5	0.249	0.626	0.624	0.565	0.565	0.578

Figure 3-5 shows the possible aspects of part Magnet. Tables 3-5 through 3-7 summarize the results of the parameters calculated and probabilities obtained by Santos for these aspects (Santos, 2004).

Figure 3-5. Natural resting aspects of part Magnet (Santos, 2004).

Table 3-5. Probability distribution: CSA method for part Magnet (Santos, 2004).

Position	Qi	hi	Qi/hi	Probability
1	6.2092	7.1172	0.87242	0.1105473
2	8.058	7.1518	1.12671	0.1427689
3	12.0064	2.0375	5.89271	0.7466839
Total	26.2736			1

Table 3-6. Probability distribution: stability method for Magnet (Santos, 2004).

Position	Ai	Hi	Ai / Hi	Probability
1	303.844	7.1172	42.6914	0.142
2	314.243	7.1518	43.939	0.14615
3	436.05	2.0375	214.012	0.71185
Total	1054.14		300.643	1

Table 3-7. Experimental Data for different vibration amplitudes per Magnet (Santos, 2004).

Positions	MDBT			MDFT		
	78%	80%	82%	78%	80%	82%
1	0.185	0.171	0.199	0.14	0.166	0.157
2	0.066	0.058	0.046	0.124	0.125	0.117
3	0.749	0.771	0.755	0.736	0.709	0.726

3.1 RESULTS

Tables 3-8 through 3-11 provide a summary of the results. Figure 3-6 is a graphical comparison of the proposed method, CSA and experimental data for "T" shape part with aspect ratio 0.6. Figure 3-7 graphs the probabilities for the different aspects on "T" shape for a range of aspects ratios. Figure 3-8 shows the experimental data and CSA method obtained for "T" shape part for the same range of aspects ratios. In the case of the "T" shape part, a nominal mass density of 9.99 E-4 grams per cubic meter was assumed in order to compute the corresponding polar moments of inertia:

The general equation used to compute the probability values was:

$$P_1 = \frac{\frac{I_1}{h_1}}{\frac{I_1}{h_1} + \frac{I_2}{h_2} + \frac{I_3}{h_3} + \frac{I_4}{h_5} + \frac{I_5}{h_5}}$$

Table 3-8. Probability distribution: Proposed method for part "T". Aspect ratio of 0.6

Aspect	Ii	hi	Ii/hi	Probability
A	402.40	14.89	27.02	0.1254
B	440.96	12.5	35.27	0.1637
C	402.40	10.11	39.8	0.1847
D	431.17	12.25	35.19	0.1633
E	586.30	7.5	78.17	0.3628
Total			215.45	0.9999

Table 3-9. Probability distribution: Proposed method for part "T"

	ASPECT RATIO					
ASPECT	0.4	0.6	0.8	1	1.2	1.4
PROBS OF "A"	9.616228	12.54201	14.75293	16.35392	17.48017	18.26498
PROBS OF "B"	12.7895	16.37167	18.92248	20.6715	21.8413	22.61887
PROBS OF "C"	14.16277	18.47186	21.7281	24.08604	25.74478	26.90065
PROBS OF "D"	12.70461	16.33489	18.95929	20.78484	22.02307	22.85728
PROBS OF "E"	50.72688	36.27959	25.6372	18.1037	12.91068	9.358216
total	100	100	100	100	100	100

Table 3-10. Probability distribution: Proposed method for part Arc Chute.

Aspect	Ii	hi	Ii/hi	Probability
1	90.80	6.87	13.21	0.1070
2	109.57	4.5	24.34	0.1971
3	109.57	4.5	24.34	0.1971
4	129.25	4.8	26.92	0.2180
5	114.75	3.31	34.66	0.2807
Total			123.47	0.9999

Table 3-11. Probability distribution: Proposed method for part Magnet.

Aspect	Ii	hi	Ii/hi	Probability
1	765.83	4.347	176.1744	0.2191
2	755.09	2.66	283.8684	0.3530
3	746.62	2.17	344.0645	0.4279
Total			804.1.73	0.9999

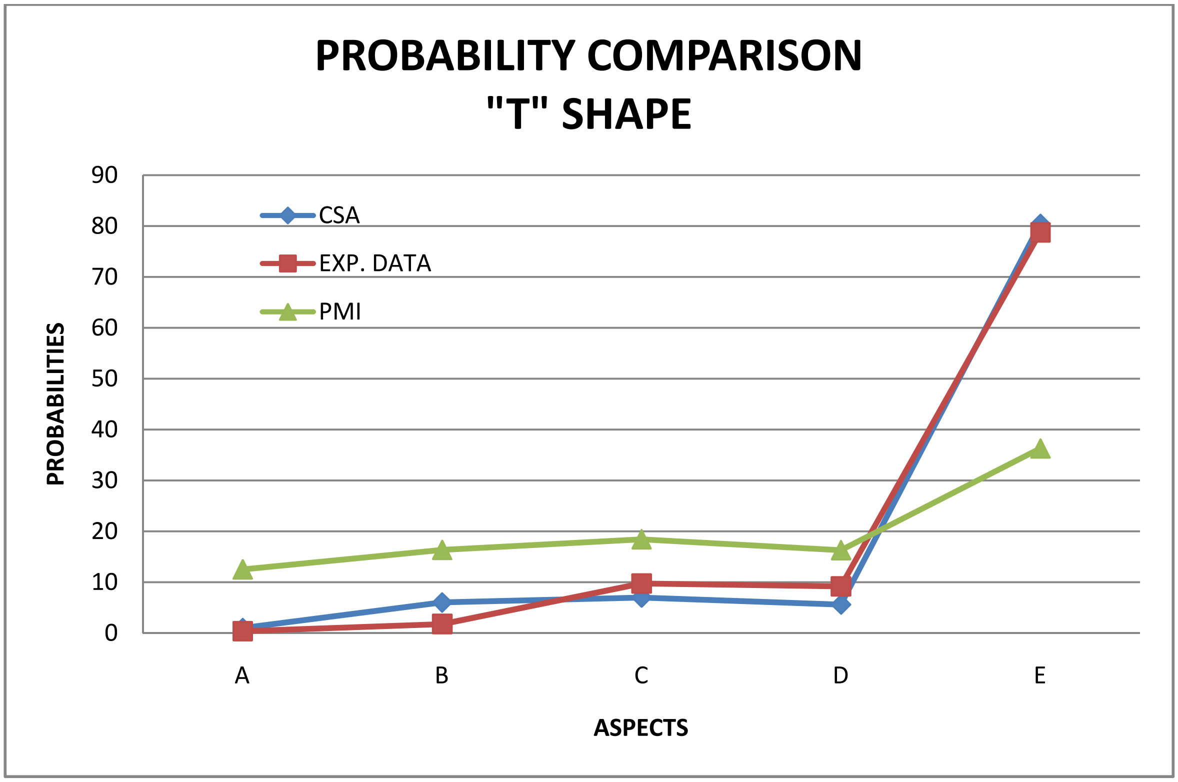

Figure 3-6. Probability comparison for "T" shape, for aspect ratio of 0.6.

In Figure 3-6 the probabilities for the different aspects of "T" shape part for an aspect ratio of 0.6 are plotted against the experimental data and the CSA method. It can be seen on Figure 3-5 that the experimental data fits well with the CSA method. The probabilities calculated with the proposed method (PMI) show differences when compared with experimental data. However, the tendency of the first four aspects on CSA probability is followed.

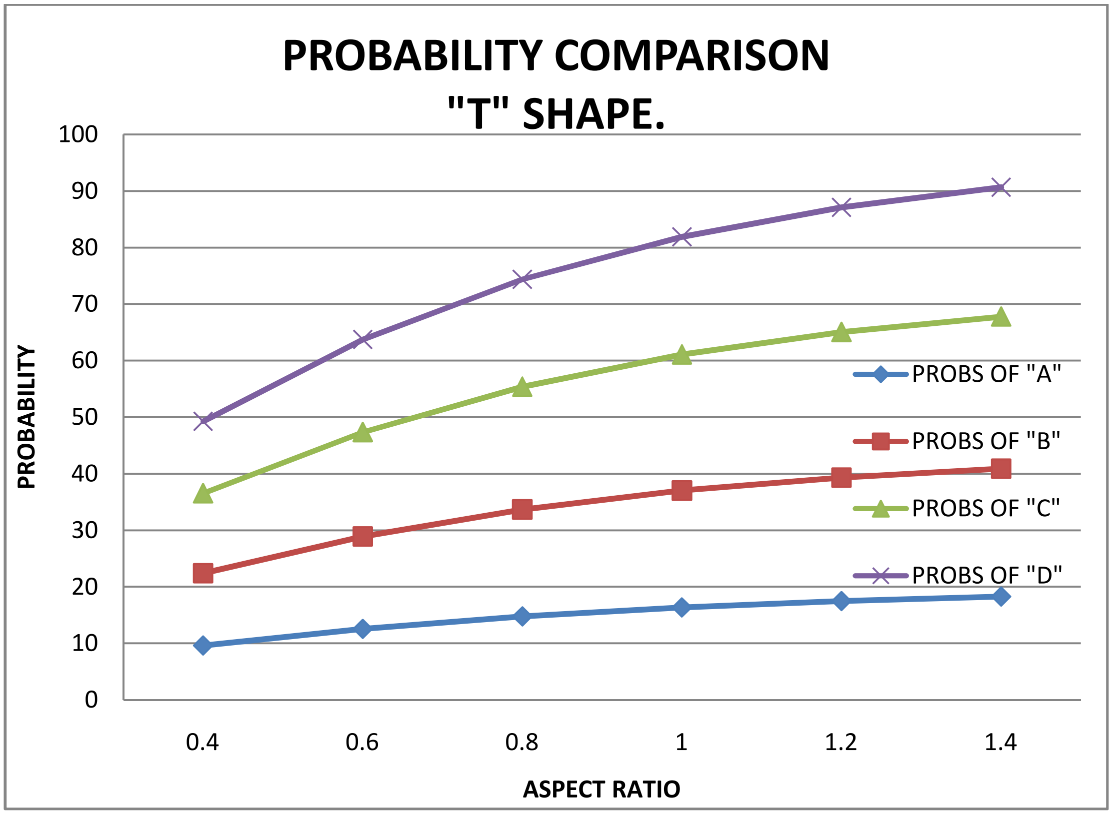

Figure 3-7. Probability distribution: Proposed method for different aspect ratio. "T" shape.

Figure 3-7 shows Ngoi's results of the probabilities for the different aspects of "T" shape part (CSA and experimental data) for aspect ratio ranging from 0.4 to of 1.4. It can be seen that the tendency of the curves are very different. The experimental data show a tendency of aspect E to dominate for small aspect ratio and to disappear for large aspect ratio. The proposed method shows the same effect but with a more relaxed curve.

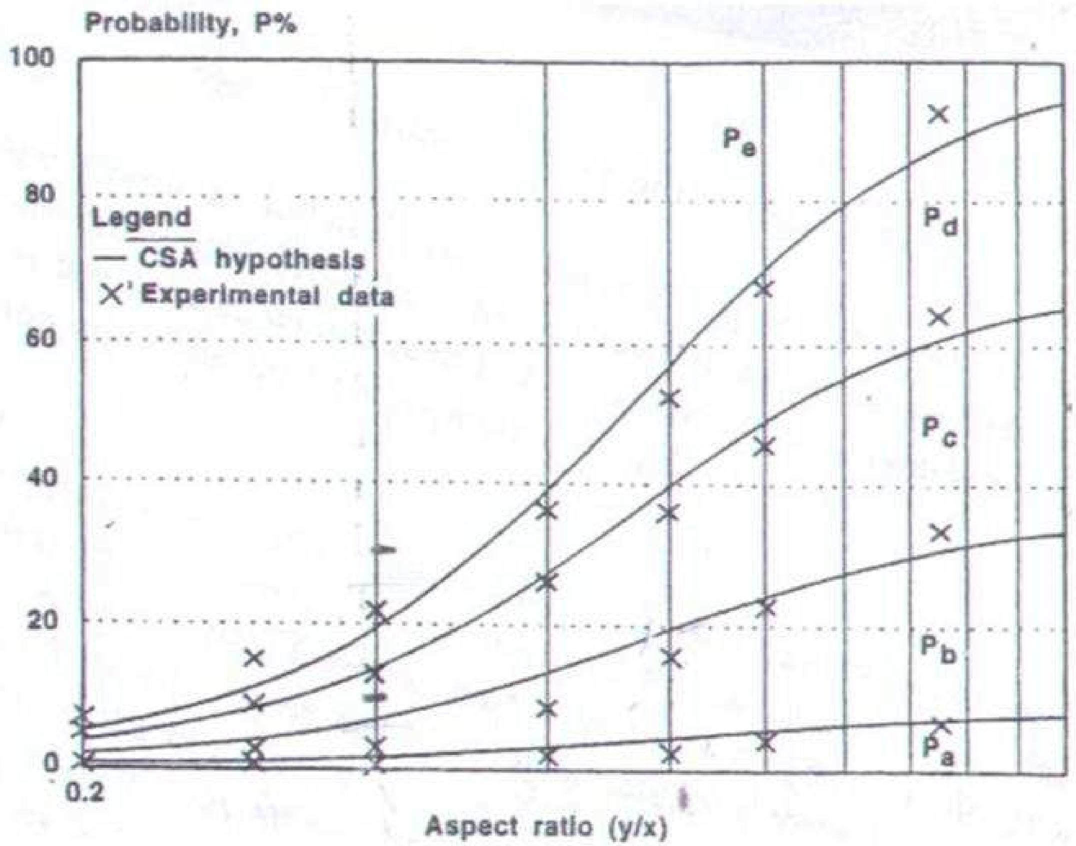

Figure 3-8. Probability distribution of the natural resting aspects of a symmetrical "T" shape prism (Ngoi, 1995-d).

In the Figures 3-9 and 3-10, the probabilities for the different aspects of Arc Chute are plotted against experimental data and the method CSA. The method has different values from experimental data, but the experimental data shows important differences between different vibration amplitudes. This condition is not supposed to happen; the data must be checked in order to have a reliable conclusion. On the other hand the method shows good probability predictions when compared against the CSA method. This is a remarkable note, because the CSA has been proved to fit with various geometries and researchers.

Figure 3-11 shows the probabilities of Arc Chute for the different aspects plotted against the Stability method; it can be seen that the predicted probabilities between the two methods are different. The values and tendencies of the proposed method and the Stability method are completely different. The same pattern is seen when comparing Stability method to CSA or experimental data. Rincon also reported poor probability predictions when comparing Stability method with CSA data for a family of parts with complex geometries (Rincon, 2002).

In the Figures 3-12 and 3-13, the probabilities for the different aspects of Magnet are plotted against experimental data and the method CSA. The PMI method has different values from experimental data. The PMI method shows good probability predictions when compared against the CSA method.

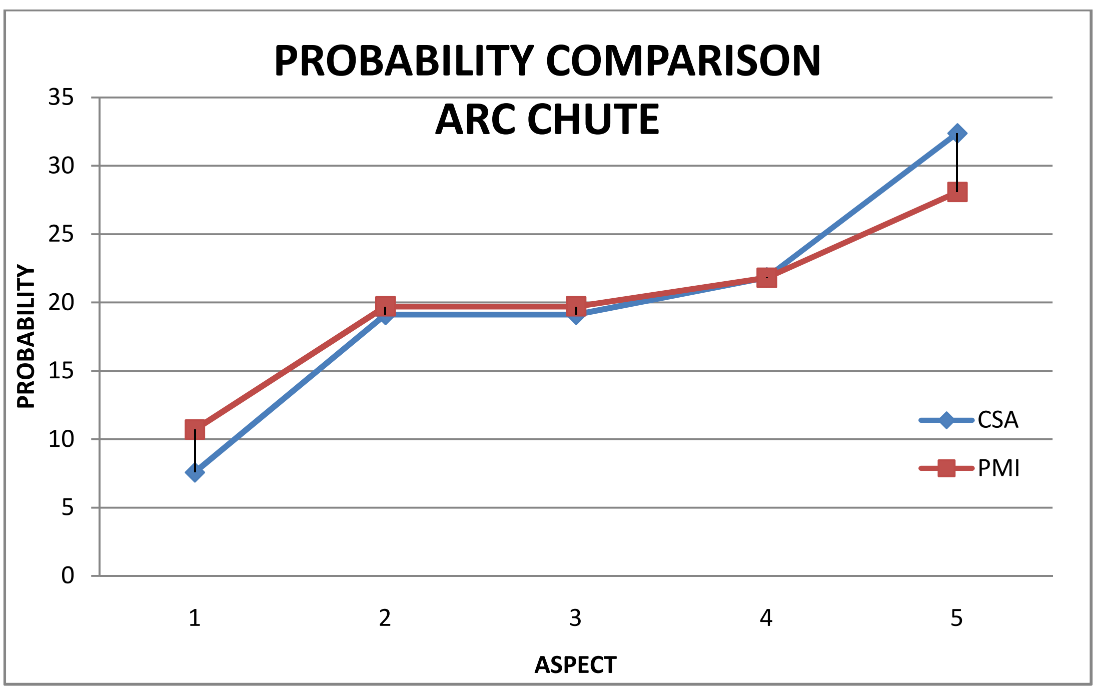

Figure 3-9. Probability comparison for Arc Chute and the CSA method.

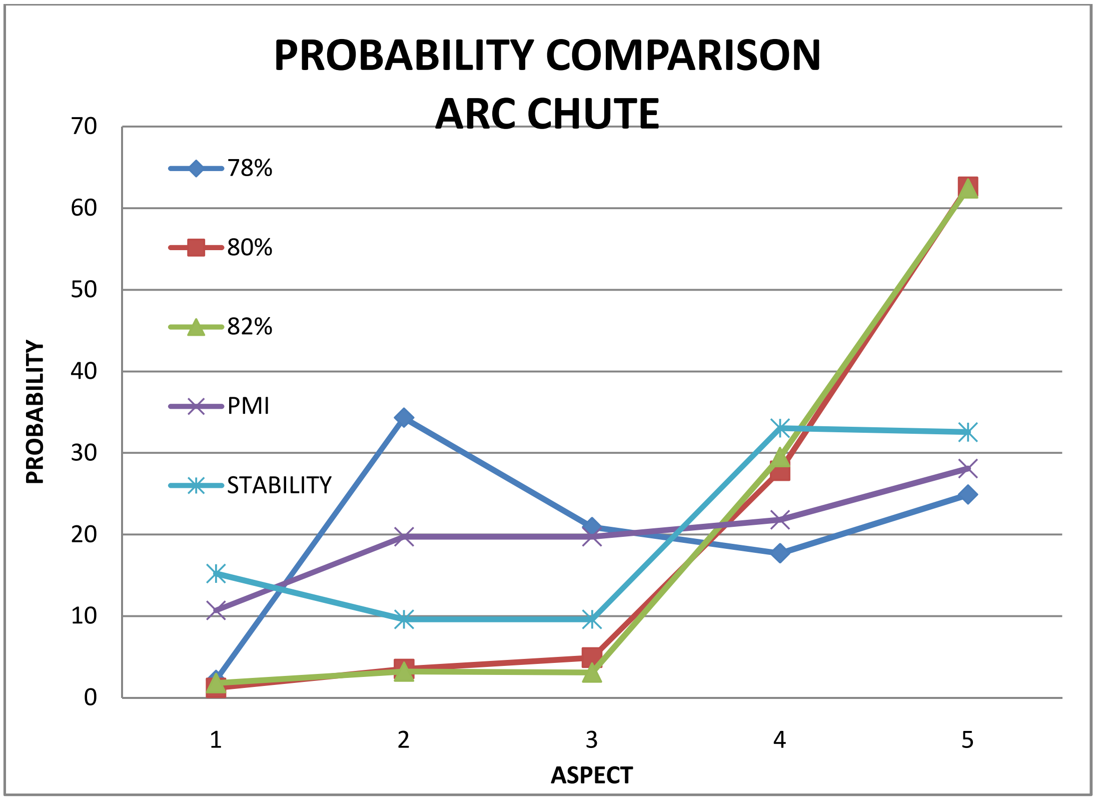

Figure 3-10. Probability comparison for Arc Chute and experimental data at different vibration amplitudes.

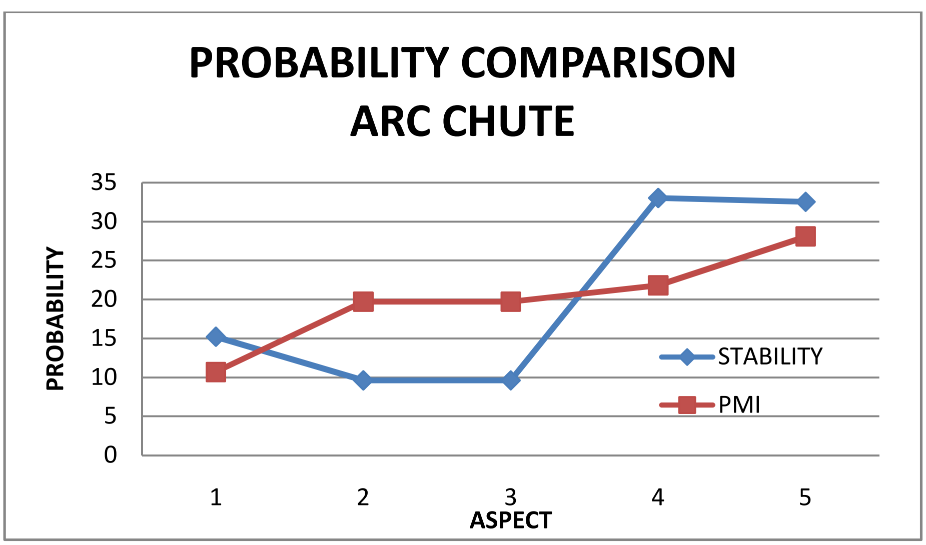

Figure 3-11. Probability comparison for Arc Chute and the Stability method.

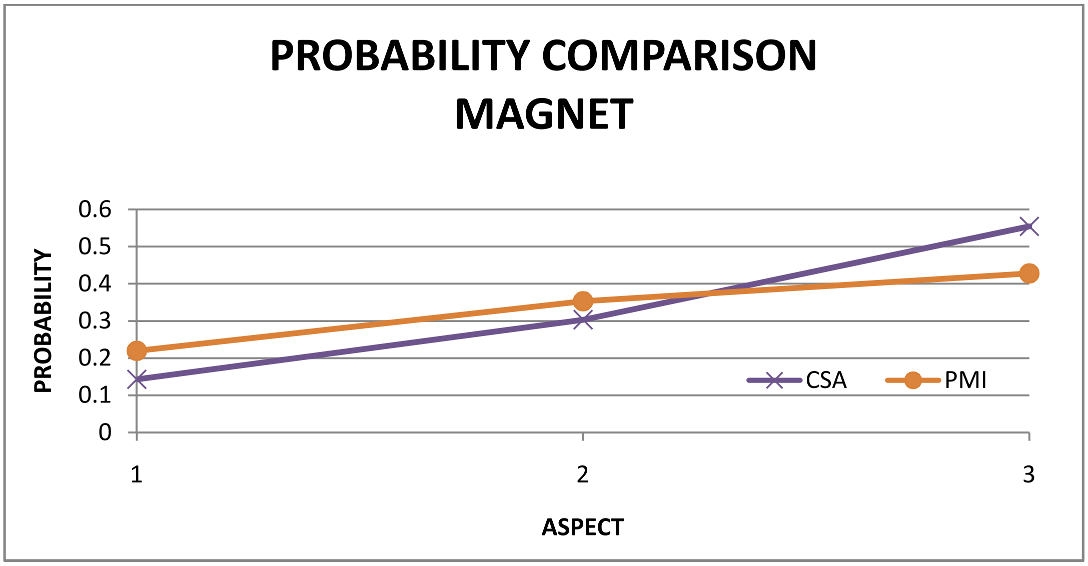

Figure 3-12. Probability comparison for Magnet and the CSA method.

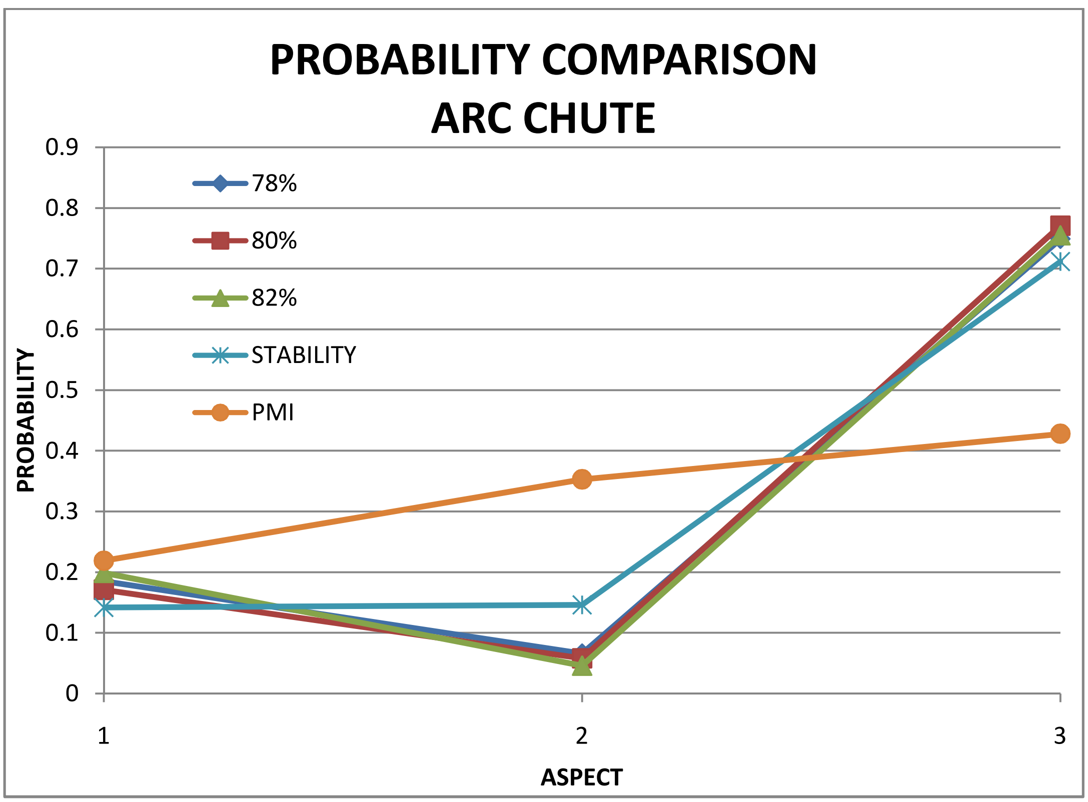

Figure 3-13. Probability comparison for Magnet and experimental data at different vibration amplitudes.

Table 3-12. Standard deviation chart per Arc Chute

SOURCE	STANDARD DEVIATION ARC CHUTE
78% - 80%	0.23
78% - 82%	0.23
78% - CSA	0.086
80% - CSA	**0.166**
78% - STABILITY	0.15
80% - STABILITY	0.15
CSA - STABILITY	0.079
78% - PMI	0.079
80% - PMI	0.189
CSA - PMI	**0.024**
STABILITY - PMI	0.085

Table 3-13. Standard deviation chart per Magnet

SOURCE	STANDARD DEVIATION MAGNET
78% - 80%	0.015
78% - 82%	0.014
78% - CSA	0.17
80% - CSA	**0.18**
78% - STABILITY	0.056
80% - STABILITY	0.063
CSA - STABILITY	0.12
78% - PMI	0.24
80% - PMI	0.26
CSA - PMI	**0.089**
STABILITY - PMI	0.2

Tables 3-12 and 3-13 shows the standard deviation between the different methods for the parts Arc Chute and Magnet; it can be seen how the deviations between PMI and CSA are acceptable.

The PMI method seems to have a good fit against the CSA method for the Arc Chute, Magnet and some aspects of the "T" shape part. However, the general tendency showed for the probabilities of resting aspects for various aspect ratios for the "T" shape demonstrate a different pattern. Similar differences can be found when comparing Arc Chute and Magnet experimental data and Stability method with PMI. The PMI still predict very well the dominant aspect over the probability profile. One possible cause for the discrepancies is the effect of product of inertia over other directions which were not accounted for. It is recommended to analyze additional parts to verify the hypothesis.

3.2 SUMMARY

In this chapter the proposed hypothesis was applied to analyze natural resting aspects of complex geometries. The also called PMI method was based in the assumption that the probability of a given aspect is directly proportional to the polar mass moment of inertia of an axis perpendicular to that aspect (measured at the center of gravity) and inversely proportional to the height of the center of gravity measured from that aspect. The PMI was applied to three different geometries and the obtained values then compared with data obtained by previous researchers. The results showed in the tables and graphics do not have the same pattern when compared with reported experimental data, even though the CSA method shows good fit for the Arc Chute, Magnet and some aspects of “T” shape part. The PMI were found valuable to predict the dominant aspect over the probability profile.

Some factors that can cause the lack of fitness are: the method does not include the effects of friction, the effects of product of inertia, the interactions between parts inside the feeder, the elastic properties of the impact surface or the effects of the feeder vibration amplitudes. The underlying premises for the method are purely geometric.

4 DYNAMIC ANALYSIS OF ARC CHUTE AND MAGNET WITH SCREW THEORY

As stated by Lipkin and Duffy, 2002: "The velocity of a rigid body is completely specified by the angular velocity vector and the linear velocity vector of an arbitrary point fixed in the body". This chapter presents the analysis of the dynamics of parts named arc chute and magnet, using Screw Theory to describe its dynamic behavior. Each part will be analyzed separately in both situations: bowl floor and bowl track. First, a set of forces acting on the parts will be reduced to a wrench. This wrench will be equalized term by term to the expression defining the time rate of change of the angular momentum screw plus screw cross product of velocity screw and momentum screw, in order to get the relationship of the main parameters governing the transport phenomena: coefficient of friction, amplitude and frequency of vibration and mass of the part.

4.1 ARC CHUTE ON BOWL BASE

The next are inertia properties of part arc chute measured at gravity center c:

$$[\mathrm{I_C}] = \begin{bmatrix} 95.32 & 0 & -24.48 \\ 0 & 109.57 & 0 \\ -24.48 & 0 & 114.75 \end{bmatrix} \mathrm{Gr.mm^2} \qquad [4.1]$$

$$\begin{bmatrix} X_C \\ Y_C \\ Z_C \end{bmatrix} = \begin{bmatrix} 3.3104 \\ 0 \\ 8.9961 \end{bmatrix} mm \qquad [4.2]$$

$$\begin{bmatrix} I_{XX} \\ I_{YY} \\ I_{ZZ} \end{bmatrix} = \begin{bmatrix} 489.45 \\ 535.01 \\ 146.06 \end{bmatrix} Gr.mm^2 \qquad \text{PART MASS=1.982 Gr.} \qquad [4.3]$$

Let P be the cross product of the velocity screw and angular momentum screw

$$\hat{S}_{P_a} = \hat{S}_{V_a} \otimes \hat{S}_{H_a} \quad [4.4]$$

The force screw will be:

$$\hat{S}_{F_A} = \left(\vec{F}_A ; \varepsilon \vec{M}_A\right) = \vec{F}_A + \varepsilon \vec{M}_A \quad [4.5]$$

By substituing equations [2.1] and [2.3] into [4.4] the screw cross product will be:

$$\hat{S}_{P_a} = \varpi \times [I_A]\varpi + \varepsilon\left(\left(\varpi \times m\left(\vec{A}\vec{G} \times \vec{V}_A\right)\right) - \left([I_A]\varpi \times \vec{V}_A\right)\right)$$

and from dual Euler equation, Newton's second law can be written as:

$$\hat{S}_{F_A} = \hat{S}_{P_A} + \frac{d\left(\hat{S}_{H_A}\right)}{dt} \quad [4.6]$$

From figure 4-1, equation [2.1] is:

$$\hat{S}_{V_C} = \begin{bmatrix} -\dot{\theta} \\ \hline 0 \\ \hline 0 \end{bmatrix} + \varepsilon \begin{bmatrix} 0 \\ \hline V_y \\ \hline V_Z \end{bmatrix} \quad [4.7]$$

The first term for angular velocity is obtained from the rotation showed on the figure. The second term for linear velocity is obtained by projecting the components of velocity vector (on XYZ system of coordinates, the point A is chosen coincident with the center of gravity) over the system of coordinates fixed in the body (X´Y´Z´) and equation [2.4] becomes:

$$\hat{S}_{H_C} = m \times \begin{bmatrix} 0 \\ \hline V_y \\ \hline V_Z \end{bmatrix} + \varepsilon[I_A] \begin{bmatrix} -\dot{\theta} \\ \hline 0 \\ \hline 0 \end{bmatrix} \quad [4.8]$$

Where I is the inertia matrix at the centroid.

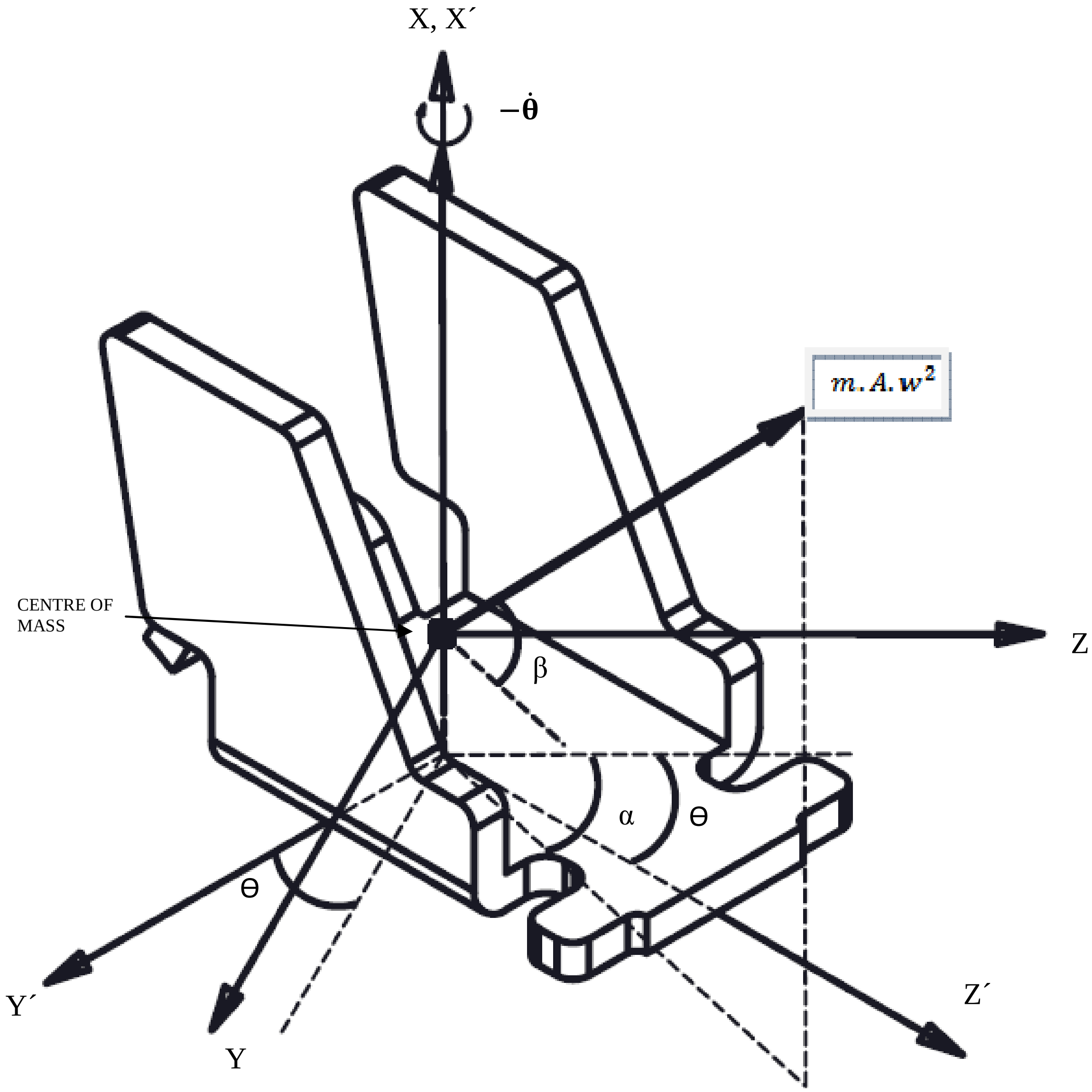

Figure 4-1. Spatial view of Arc Chute on bowl floor.

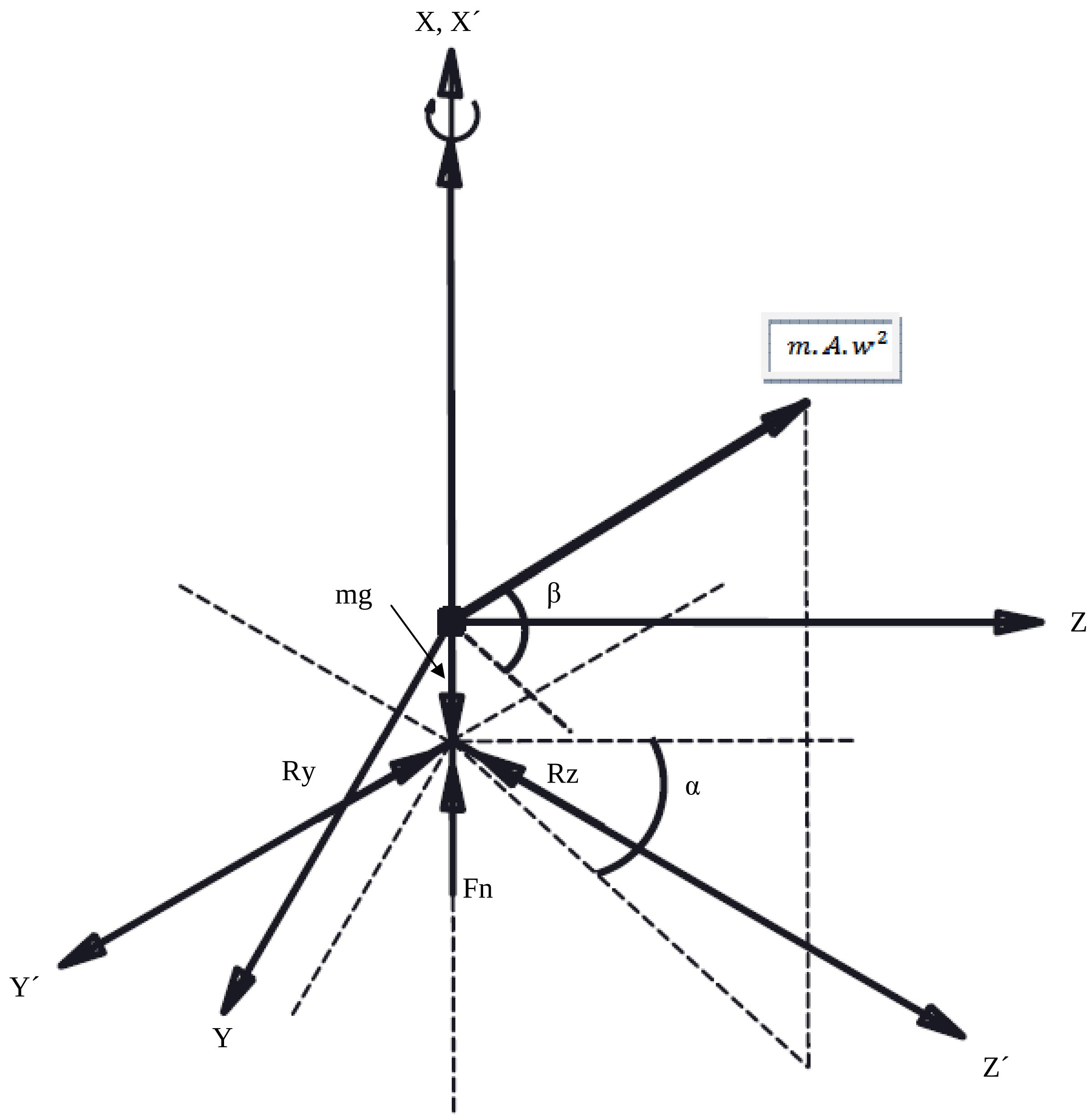

Figure 4-2. Forces acting on Arc Chute.

After substituting [4.1], [4.2] and [4.5], [4.4] becomes:

$$\hat{S}_{P_C} = m_C \times \begin{bmatrix} 0 \\ \dot{\theta}(V_Z) \\ -\dot{\theta}(V_y) \end{bmatrix} + \varepsilon \begin{bmatrix} 0 \\ -(I_{ZX})\dot{\theta}^2 \\ 0 \end{bmatrix} \qquad [4.9]$$

The first term of [4.9] is obtained by performing the operation screw cross products between the velocity and momentum screws.

The time derivative of [4.8] is:

$$\frac{d}{dt}\left[\hat{S}_{H_C}\right] = m_C \times \begin{bmatrix} 0 \\ \hline \dot{V}_y \\ \hline \dot{V}_Z \end{bmatrix} + \varepsilon \begin{bmatrix} -(I_{XX})\ddot{\theta} \\ \hline 0 \\ \hline -(I_{ZX})\ddot{\theta} \end{bmatrix} \qquad [4.10]$$

$$\hat{S}_{FC} = \hat{S}_{PC} + \frac{d}{dt}\hat{S}_{HC} \qquad [4.11]$$

Adding [4.9] and [4.10], [4.11] is:

$$\hat{S}_{F_C} = m_C \begin{bmatrix} 0 \\ \hline \left(\dot{V}_y + V_Z \times \dot{\theta}\right) \\ \hline \left(\dot{V}_Z - V_y \times \dot{\theta}\right) \end{bmatrix} + \varepsilon \begin{bmatrix} -(I_{XX})\ddot{\theta} \\ \hline -(I_{ZX})\dot{\theta}^2 \\ \hline -(I_{ZX})\ddot{\theta} \end{bmatrix} \qquad [4.12]$$

Then, from figure 4.2 the acting forces on the body including its own weight and vibration force, are:

$$\hat{S}_{F_C} = \begin{bmatrix} + mA\omega^2 \sin(\beta) + (F_N \ - m \times g) \\ \hline mA\omega^2 (\cos(\beta)\left(-\cos\alpha \sin\theta + \sin\alpha \cos\theta\right) - R_y \\ \hline mA\omega^2 (\cos(\beta)\left(\cos\alpha \cos\theta + \sin\alpha \sin\theta\right) - R_z \end{bmatrix}$$
$$+ \varepsilon \begin{bmatrix} -3.15mA\omega^2 \cos(\beta)\sin(\alpha-\theta) \\ \hline -3.31R_Z + d \times F_N + \cos(\theta)(3.15(mA\omega^2 \sin(\beta) + 3.31mA\omega^2 \cos(\beta)\cos(\alpha)) \\ \hline +3.31R_y - \sin(\theta)(3.15mA\omega^2 \sin(\beta) + 3.31mA\omega^2 \cos(\beta)\cos(\alpha)) \end{bmatrix} \qquad [4.13]$$

Equation [4.13] is obtained projecting the components of the acting forces which are: the parts weight, the bowl force, and the normal, friction and reaction forces over the three axes. The components not acting directly on the centre of mass are translated there compensating with an equivalent moment. Equation [4.13] corresponds to the components of the real and dual parts in the three body axes, named X´, Y´, and Z´.

To proceed, the real and dual components are equal to:

REAL PART:

$$\begin{aligned} &+\mathrm{mA}\omega^2\sin(\beta)+(\mathrm{F_N}-\mathrm{m}\times\mathrm{g})=0 \\ &\mathrm{F_N} = -\mathrm{mA}\omega^2\sin(\beta)+\mathrm{m}\times\mathrm{g} \end{aligned} \qquad [4.14]$$

$$\mathrm{m}(\dot{\mathrm{V}}_{\mathrm{y}}-\mathrm{V_Z}\,\dot{\theta})=\mathrm{mA}\omega^2(\cos(\beta)\left(-\cos\alpha\sin\theta+\sin\alpha\cos\theta\right)-\mathrm{R_y} \qquad [4.15]$$

$$\mathrm{m}(\dot{\mathrm{V}}_{\mathrm{Z}}+\mathrm{V_y}\,\dot{\theta})=\mathrm{mA}\omega^2(\cos(\beta)\left(\cos\alpha\cos\theta+\sin\alpha\sin\theta\right)-\mathrm{R_z} \qquad [4.16]$$

DUAL PART:

$$-95.32\times\ddot{\theta}=-3.15\mathrm{mA}\omega^2\cos(\beta)\sin(\alpha-\theta) \qquad [4.17]$$

$$\begin{aligned} &-3.31\mathrm{R_Z}+\mathrm{d}\times\mathrm{F_N}+\cos\theta(3.15\mathrm{mA}\omega^2\sin(\beta) \\ &+3.31\mathrm{mA}\omega^2\cos(\beta)\cos(\alpha))=24.48\times\dot{\theta}^2 \end{aligned} \qquad [4.18]$$

$$3.31\mathrm{R_y}-\sin\theta(3.15\mathrm{mA}\omega^2\sin(\beta)+3.31\mathrm{mA}\omega^2\cos(\beta)\cos(\alpha))=24.48\times\ddot{\theta} \quad [4.19]$$

Solving the resultant system of equations leads to:

With the aid of Equations [4.14] through [4.16]

$$F_N = -mA\omega^2(\sin(\beta) + m \times g \qquad [4.20]$$

$$\dot{V}_Y = A\omega^2(\cos(\beta)\sin(\alpha-\theta)) - \frac{R_y}{m} + V_Z\,\dot{\theta} \qquad [4.21]$$

$$\dot{V}_Z = A\omega^2(\cos(\beta)\cos(\alpha-\theta)) - \frac{R_z}{m} - V_y\,\dot{\theta} \qquad [4.22]$$

With the aid of [4.17], [4.18] and the fact that the normal surface reaction will compensate for any rotation about the Y axis, the angular acceleration and velocity are:

$$\left|\ddot{\theta}\right| = 0.033 \times mA\omega^2 \cos(\beta)\sin(\alpha-\theta) \qquad [4.23]$$

$$\dot{\theta} = 0 \qquad [4.24]$$

The obtained results suggest that because the angles α and β (alpha and beta) are prescribed by the bowl feeder, the part will always have an angular acceleration $\ddot{\theta}$ around the X axis, which is not desirable for the transportation phenomena. Therefore, the stability cannot be achieved unless another constraint is imposed.

This condition will hold except for the case where the angle α and θ (alpha and theta) have equal value. In this case $\ddot{\theta} = 0$, $\dot{\theta} = 0$ and the part will translate with no rotation.

For this case, the sliding along the Y axis does not occur, the tangential component of the displacement becomes cero along with the correspondent friction component.

The limiting condition is given by:

$$\mathrm{A}\omega^2(\cos(\beta)\cos(\alpha-\theta))-\mathrm{R}_Z\rangle 0 \qquad [4.25]$$

For this case the Coulomb friction law is applicable having:

$$R_Z = \mu_K F_N \qquad [4.26]$$

Replacing the equations [4.20], [4.25] and [4.26], the limiting condition can be found as:

$$\mu\langle\frac{\mathrm{A}\omega^2(\cos(\beta)\cos(\alpha-\theta))}{\left[\mathrm{g}-\mathrm{A}\omega^2\sin(\beta)\right]} \qquad [4.27]$$

And the boundary is given by [4.28]

$$\mu=\frac{\mathrm{A}\omega^2(\cos(\beta))}{\left[\mathrm{g}-\mathrm{A}\omega^2\sin(\beta)\right]} \qquad [4.28]$$

4.2 ARC CHUTE ON BOWL TRACK

In this section, the arc chute will be analyzed on the narrow track by reducing the set of forces to a wrench and then equaling the resultant expression to the time rate of change of the angular momentum screw plus the cross product of velocity and momentum screw, in order to get the main parameters governing the transport phenomena. In this case the forces and reactions are affected by the three track angles: one on X-Z plane because the bowl radius, and two on Y-Z, X-Z planes, because the track inclination. Axes X and Z will be switched to manage those new conditions.

Figures 4-3, 4-4 and 4-5 show the acting forces on the body, including its own weight and vibration force. The forces R_{1f} and R_{2f} (not indicated in the drawings) referred in the equations are the friction forces due to the normal reactions R_1 and R_2. By projecting this set of forces over the three axes, taking account on the inclination and vibration angle, the force screw will be:

$$\hat{S}_{F_C} = \begin{bmatrix} R_1\sin(\sigma) - R_2\sin(\sigma) + mA\omega^2\cos(\beta)\cos(\alpha-\theta) - m\times g\sin(\varphi) \\ -R_{1f} - R_{2f} - R_4 \\ \hline R_1\cos(\sigma)\cos(\delta) + R_2\cos(\sigma)\cos(\delta) \\ + mA\omega^2(\cos(\beta)\sin(\alpha-\theta)\cos(\delta) + \sin(\beta)\sin(\delta)) + R_3 \\ \hline + F_N - m\times g\cos(\varphi)\cos(\delta) - R_1\cos(\sigma)\sin(\delta) - R_2\cos(\sigma)\sin(\delta) \\ + mA\omega^2(\sin(\beta)\cos(\delta) - \cos(\beta)\sin(\alpha-\theta)\sin(\delta)) \end{bmatrix}$$

$$+\varepsilon\begin{bmatrix} \\ -3.3104\times R_3 + 8.01\times\sin(64.22-\delta)\cos(\sigma)(R_1+R_2) \\ \hline -3.31\times R_4 + 8.01\times\sin(64.22-\delta)\sin(\sigma)(R_2-R_1)\cos(\delta) + 4.05\sin(\sigma)(R_2-R_1)\sin(\delta) \\ + (6.7R_1 - 8.99R_2)\cos(\sigma)\sin(\delta) + 4.01(R_{1f}+R_{2f})\sin(\delta) + d\times F_N \\ + mA\omega^2(3.15\sin(\beta)\cos(\delta) + 3.31\cos(\beta)\cos(\alpha-\theta)\cos(\delta) - 3.15\cos(\beta)\sin(\alpha-\theta)\sin(\delta)) \\ \hline - mA\omega^2(3.15\sin(\beta)\sin(\delta) + 3.31\cos(\beta)\cos(\alpha-\theta)\sin(\delta) + 3.15\cos(\beta)\sin(\alpha-\theta)\cos(\delta)) \\ -8.01\times\sin(64.22-\delta)\sin(\sigma)(R_2-R_1)\sin(\delta) + 4.05\sin(\sigma)(R_2-R_1)\cos(\delta) \\ + (6.7R_1 - 8.99R_2)\cos(\sigma)\cos(\delta) + 4.01(R_{1f}+R_{2f})\cos(\delta) \end{bmatrix}$$

[4.29]

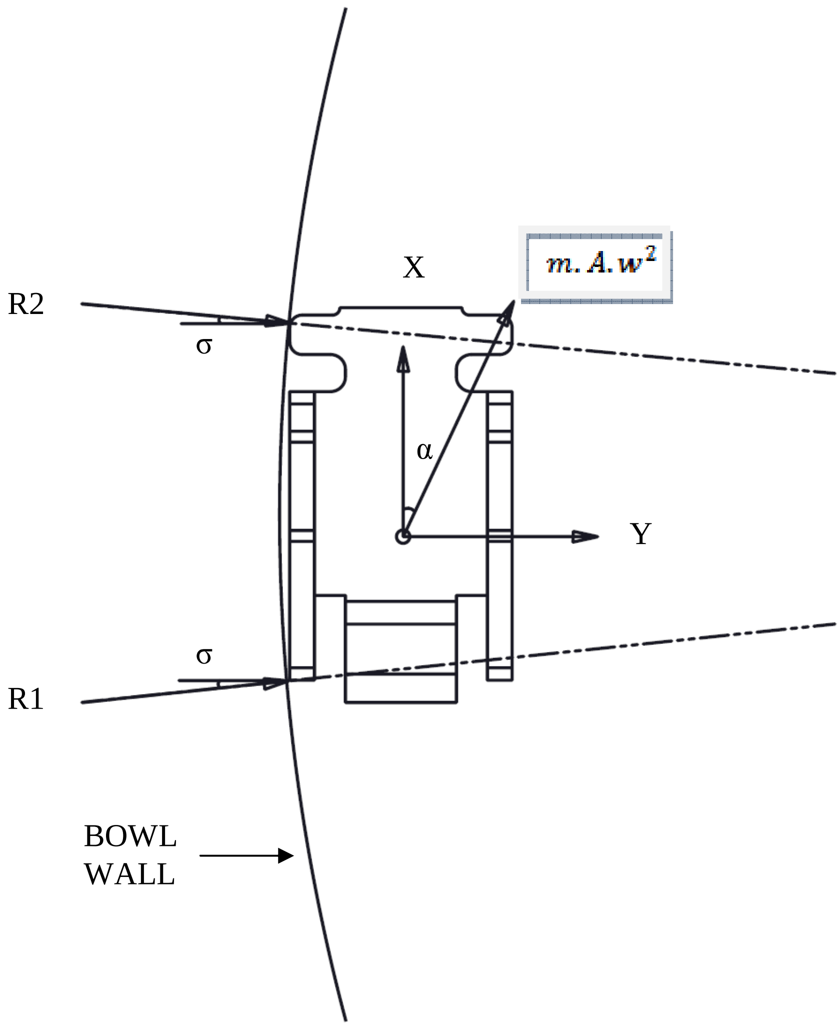

Figure 4-3. Arc Chute top view on bowl track

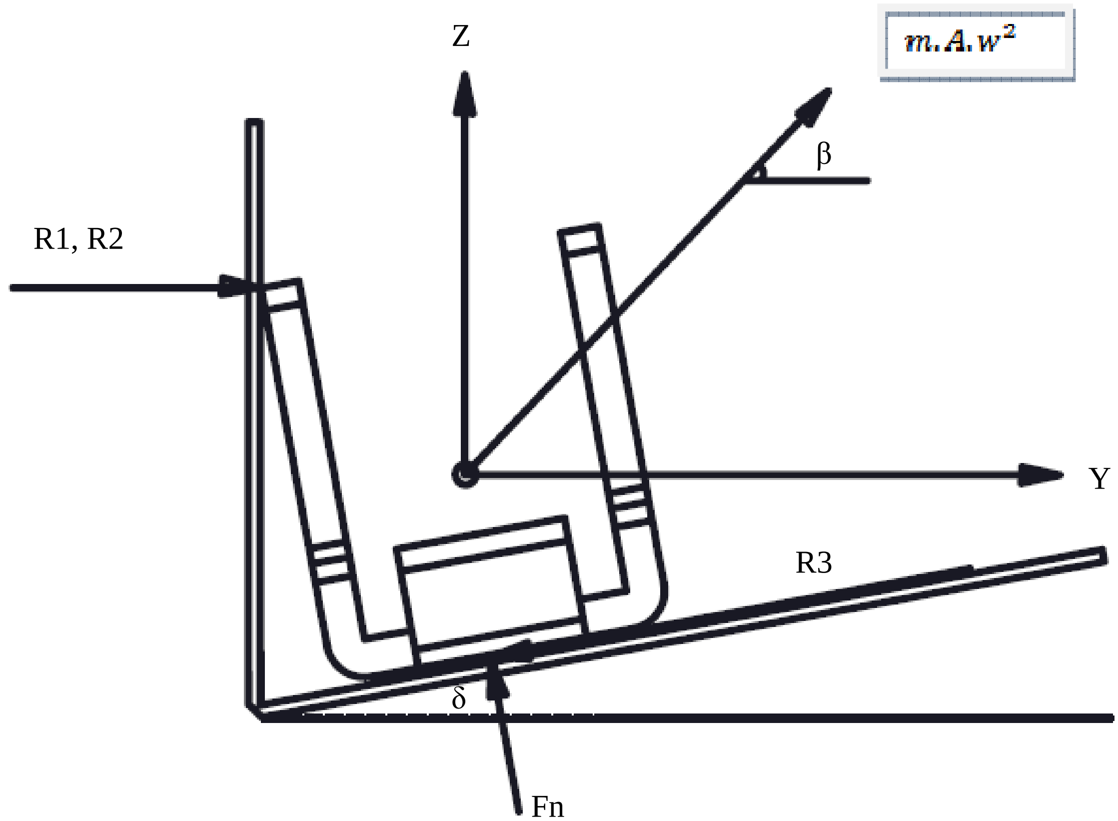

Figure 4-4. Arc Chute rear view on bowl track

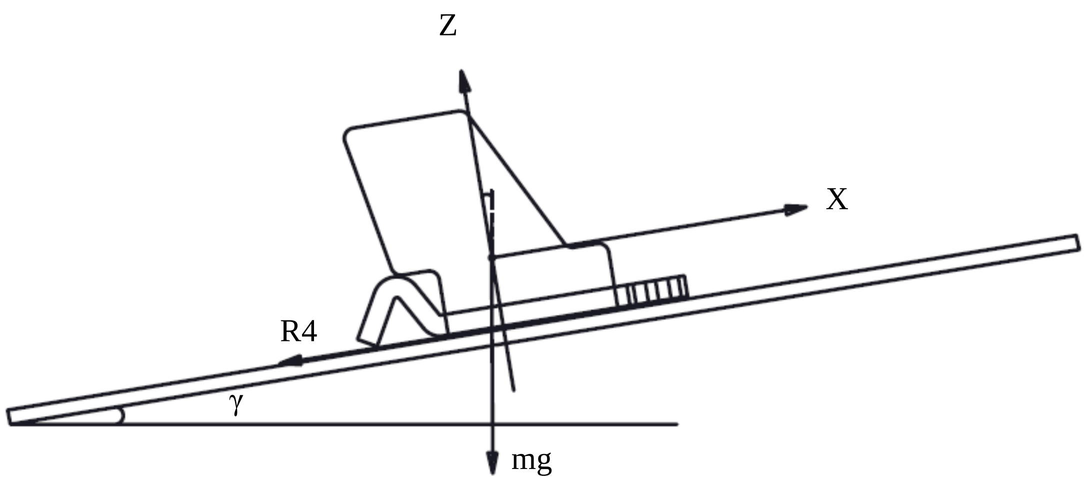

Figure 4-5. Arc Chute side view on bowl track

Equation [4.29] corresponds to the components of the real and dual parts in the three axes, named X, Y, Z.

Then, the axis will be switched, X to Z as related before, equation [4.10] becomes:

$$\frac{d}{dt}\left[\hat{S}_{H_C}\right] = m_C \times \begin{bmatrix} \dot{V}_x \\ \dot{V}_y \\ 0 \end{bmatrix} + \varepsilon \begin{bmatrix} -(I_{ZX})\ddot{\theta} \\ 0 \\ -(I_{XX})\ddot{\theta} \end{bmatrix} \qquad [4.30]$$

And [4.12] becomes:

$$\hat{S}_{F_C} = \hat{S}_{P_C} + \frac{d}{dt}\hat{S}_{H_C} = m_C \begin{bmatrix} \dot{V}_X + V_Y\dot{\theta} \\ \dot{V}_y - V_X\dot{\theta} \\ 0 \end{bmatrix} + \varepsilon \times [I_C] \begin{bmatrix} -(I_{ZX})\ddot{\theta} \\ -(I_{ZX})\dot{\theta}^2 \\ -(I_{XX})\ddot{\theta} \end{bmatrix} \qquad [4.31]$$

To proceed, the real and dual components are equal to:

REAL PART:

$$m_C(\dot{V}_X + V_Y\dot{\theta}) = R_1\sin(\sigma) - R_2\sin(\sigma) + mA\omega^2\cos(\beta)\cos(\alpha-\theta) - m\times g\sin(\varphi) - R_{1f} - R_{2f} - R_4 \qquad [4.32]$$

$$m_C(\dot{V}_y - V_X\dot{\theta}) = R_1\cos(\sigma)\cos(\delta) + R_2\cos(\sigma)\cos(\delta) + mA\omega^2(\cos(\beta)\sin(\alpha-\theta)\cos(\delta) + \sin(\beta)\sin(\delta)) + R_3 \qquad [4.33]$$

$$0 = +F_N - m\times g\cos(\varphi)\cos(\delta) - R_1\cos(\sigma)\sin(\delta) - R_2\cos(\sigma)\sin(\delta) + mA\omega^2(\sin(\beta)\cos(\delta) - \cos(\beta)\sin(\alpha-\theta)\sin(\delta)) \qquad [4.34]$$

DUAL PART:

$$-3.3104\times R_3 + 8.01\times\sin(64.22-\delta)\cos(\sigma)(R_1 + R_2) = 24.48\ddot{\theta} \qquad [4.35]$$

$$
\begin{aligned}
&-3.31\times R_4 + 8.01\times \sin(64.22-\delta)\sin(\sigma)(R_2 - R_1)\cos(\delta)\\
&+4.05\sin(\sigma)(R_2 - R_1)\sin(\delta) + (6.7R_1 - 8.99R_2)\cos(\sigma)\sin(\delta)\\
&+4.01(R_{1f} + R_{2f})\sin(\delta) + d\times F_N + mA\omega^2(3.15\sin(\beta)\cos(\delta)\\
&+3.31\cos(\beta)\cos(\alpha-\theta)\cos(\delta) - 3.15\cos(\beta)\sin(\alpha-\theta)\sin(\delta)) = 24.48\times\dot{\theta}^2
\end{aligned}
\qquad [4.36]
$$

$$
\begin{aligned}
&-mA\omega^2(3.15\sin(\beta)\sin(\delta) + 3.31\cos(\beta)\cos(\alpha-\theta)\sin(\delta)\\
&+3.15\cos(\beta)\sin(\alpha-\theta)\cos(\delta)) - 8.01\times\sin(64.22-\delta)\sin(\sigma)(R_2 - R_1)\sin(\delta)\\
&+4.05\sin(\sigma)(R_2 - R_1)\cos(\delta) + (6.7R_1 - 8.99R_2)\cos(\sigma)\cos(\delta)\\
&+4.01(R_{1f} + R_{2f})\cos(\delta) = -95.32\ddot{\theta}
\end{aligned}
$$

[4.37]

The bowl wall constrains rotation about the Z axis, (we assume that the part and bowl wall keep in contact at all times) having $\ddot{\theta} = 0$

The obtained results suggests that if the angle δ is equal to 64.44 the reaction R_3 will be zero, so there would not be displacement in the Y (radial) direction. This condition is expected for a forward conveying. In this case the bowl wall prevents the rotation around the Z axis, which is a desirable stability condition for the part.

4.3 MAGNET ON BOWL BASE

The next are inertia properties of part magnet measured at gravity center **c**

$$
[I_C] = \begin{bmatrix} 755.91 & 10.91 & 0 \\ -10.91 & 755.09 & 0 \\ 0 & 0 & 49.92 \end{bmatrix} \text{Gr.mm}^2
$$

$$
\begin{bmatrix} X_C \\ Y_C \\ Z_C \end{bmatrix} = \begin{bmatrix} 2.16 \\ 2.66 \\ 25.68 \end{bmatrix} \text{mm}
$$

PART MASS=4.63 Gr.

From figure 4-6, equation [2.1] is:

$$\hat{S}_{V_C} = \begin{bmatrix} -\dot{\theta} \\ \hline 0 \\ \hline 0 \end{bmatrix} + \varepsilon \begin{bmatrix} 0 \\ \hline V_y \\ \hline V_Z \end{bmatrix} \qquad [4.38]$$

As related for the Arc Chute, the first term for angular velocity is obtained from the rotations showed on the figure. The second term for linear velocity is obtained by projecting the components of velocity vector (on XYZ system of coordinates) over the system of coordinates fixed in the body (X´Y´Z´). In the following equations the principal screw of inertia in the direction Z was supposed to be in the same direction of the axis showed in the Figure 4-6, even though it is not exactly coincident for the part, but the angle deviation is four degrees which was not consider a significant change. Equation [2.4] becomes:

$$\hat{S}_{H_C} = m \times \begin{bmatrix} 0 \\ \hline V_y \\ \hline V_Z \end{bmatrix} + \varepsilon [I] \begin{bmatrix} -\dot{\theta} \\ \hline 0 \\ \hline 0 \end{bmatrix} \qquad [4.39]$$

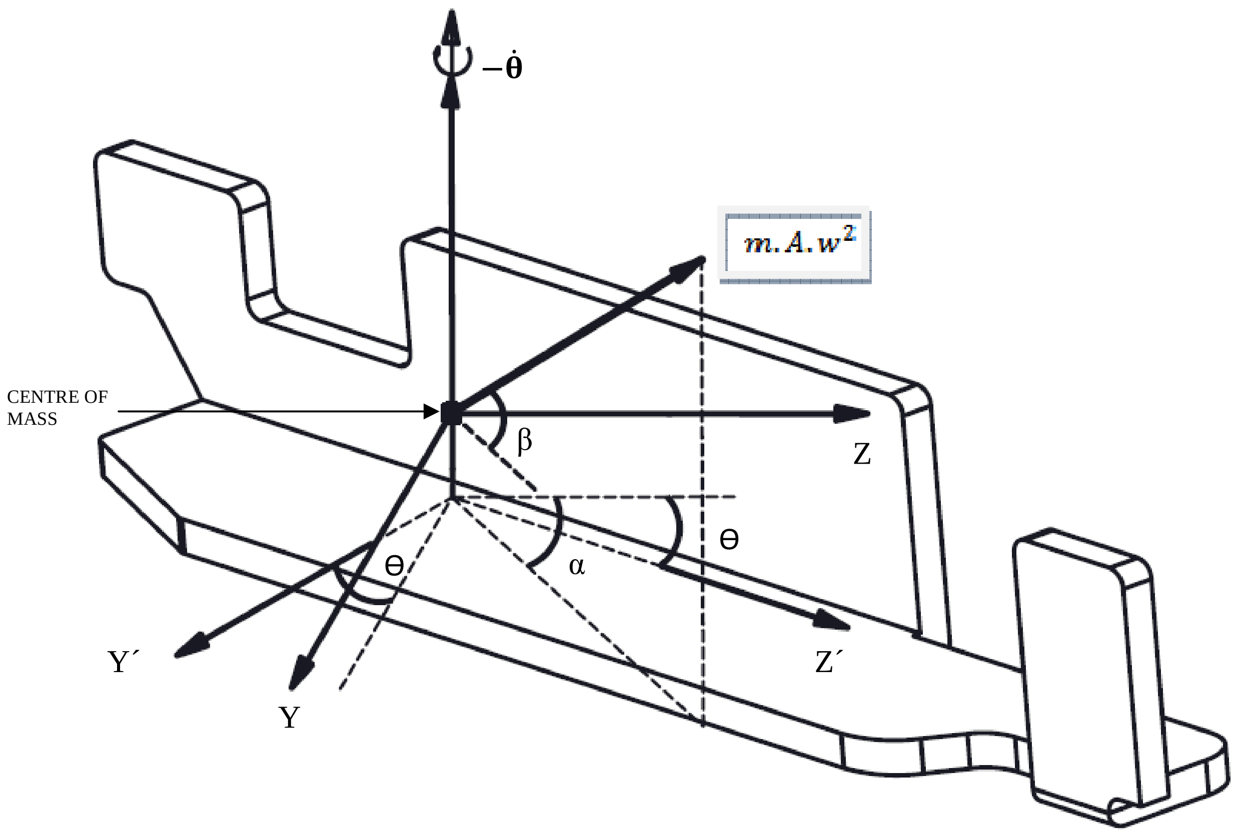

Figure 4-6. Spatial view of Magnet on bowl floor.

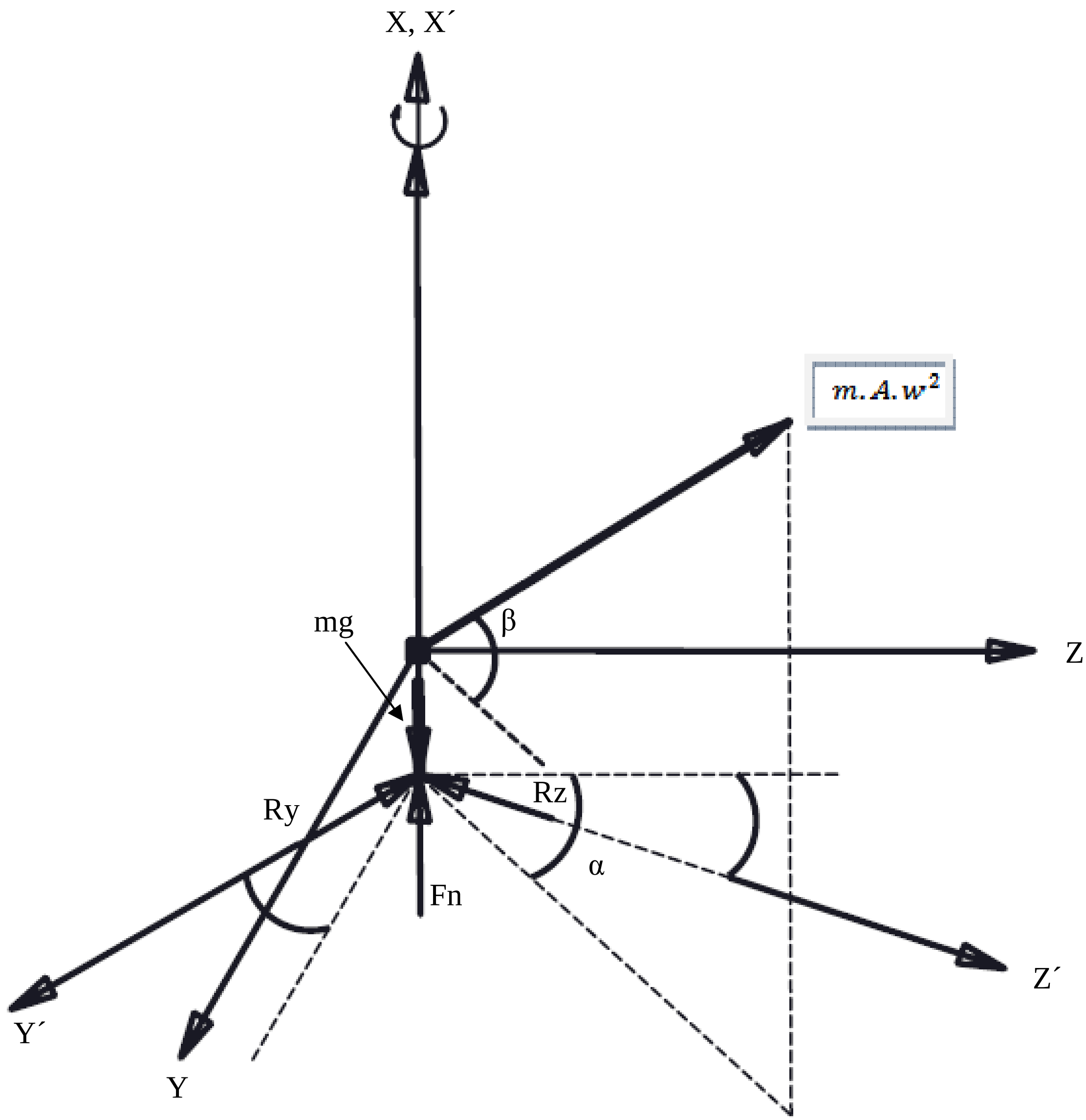

Figure 4-7. Forces acting on magnet.

Equation, [4.9] remains the same:

$$\hat{S}_{P_C} = m_C \times \left[\begin{array}{c} 0 \\ \hline \dot{\theta}(V_Z) \\ \hline -\dot{\theta}(V_y) \end{array} \right] + \varepsilon \left[\begin{array}{c} 0 \\ \hline 0 \\ \hline (I_{YX})\dot{\theta}^2 \end{array} \right] \qquad [4.40]$$

The first term of [4.40] is obtained is obtained by performing the operation screw cross products between the velocity and momentum screws.

The time derivative of [4.39] is:

$$\frac{d}{dt}\left[\hat{S}_{H_C}\right] = m_C \times \begin{bmatrix} 0 \\ \hline \dot{V}_y \\ \hline \dot{V}_Z \end{bmatrix} + \varepsilon\left[I_C\right] \begin{bmatrix} -(I_{XX})\ddot{\theta} \\ \hline -(I_{YX})\ddot{\theta} \\ \hline 0 \end{bmatrix} \qquad [4.41]$$

$$\hat{S}_{FC} = \hat{S}_{PC} + \frac{d}{dt}\hat{S}_{HC}$$

Adding [4.40] and [4.41], [4.11] becomes:

$$\hat{S}_{F_C} = m_C \begin{bmatrix} 0 \\ \hline \left(\dot{V}_y + V_Z \times \dot{\theta}\right) \\ \hline \left(\dot{V}_Z - V_y \times \dot{\theta}\right) \end{bmatrix} + \varepsilon\left[I_C\right] \begin{bmatrix} -(I_{XX})\ddot{\theta} \\ \hline -(I_{YX})\ddot{\theta} \\ \hline (I_{YX})\dot{\theta}^2 \end{bmatrix} \qquad [4.42]$$

Then from figure 4.7 the acting forces on the body including its own weight and vibration force, we have:

$$\hat{S}_{F_C} = \begin{bmatrix} + mA\omega^2(\sin(\beta)) + (F_N \ - m \times g) \\ \hline mA\omega^2(\cos(\beta)(-\cos\alpha\sin\theta + \sin\alpha\cos\theta) - R_y \\ \hline mA\omega^2(\cos(\beta)(\cos\alpha\cos\theta - \sin\alpha\sin\theta) - R_z \end{bmatrix}$$

$$+\varepsilon\begin{bmatrix}-2.82\mathrm{mA}\omega^2\cos(\beta)\sin(\alpha-\theta)\\ \hline -2.16\mathrm{R}_Z+\mathrm{d}\times\mathrm{F}_\mathrm{N}+\cos(\theta)(2.82\mathrm{mA}\omega^2\sin(\beta)+2.16\mathrm{mA}\omega^2\cos(\beta)\cos(\alpha))\\ \hline +2.16\mathrm{R}_y-\sin(\theta)(2.82\mathrm{mA}\omega^2\sin(\beta)+2.16\mathrm{mA}\omega^2\cos(\beta)\cos(\alpha))\end{bmatrix} \quad [4.43]$$

Equation [4.43] is obtained projecting the components of the acting forces which are: the parts weight, the bowl force, and the normal, friction and reaction forces over the three body fixed axes. The components not acting directly on the centre of mass are translated there compensating with an equivalent moment.

Equation [4.43] corresponds to the components of the real and dual parts in the three axes, named X´, Y´, and Z´.

To proceed, the real and dual components are equal to:

REAL PART:

$$+\mathrm{mA}\omega^2(\sin(\beta))+(\mathrm{F}_\mathrm{N}-\mathrm{m}\times\mathrm{g})=0$$

$$\mathrm{F}_\mathrm{N}=-\mathrm{mA}\omega^2(\sin(\beta))+\mathrm{m}\times\mathrm{g} \quad [4.44]$$

$$\mathrm{mA}\omega^2(\cos(\beta)(-\cos\alpha\sin\theta+\sin\alpha\cos\theta)-\mathrm{R}_y=\dot{\mathrm{V}}_y+\mathrm{V}_Z\times\dot{\theta} \quad [4.45]$$

$$\mathrm{mA}\omega^2(\cos(\beta)(\cos\alpha\cos\theta-\sin\alpha\sin\theta)-\mathrm{R}_z=\dot{\mathrm{V}}_Z-\mathrm{V}_y\times\dot{\theta} \quad [4.46]$$

DUAL PART:

$$-755.91\times\ddot{\theta}=-2.82\mathrm{mA}\omega^2\cos(\beta)\sin(\alpha-\theta) \quad [4.47]$$

$$10.91\times\ddot{\theta}=-2.16\mathrm{R}_Z+\mathrm{d}\times\mathrm{F}_\mathrm{N}+\cos(\theta)(2.82\mathrm{mA}\omega^2\sin(\beta)+2.16\mathrm{mA}\omega^2\cos(\beta)\cos(\alpha)) \quad [4.48]$$

$$-10.91\times\dot{\theta}^2=2.16\mathrm{R}_y-\sin(\theta)(2.82\mathrm{mA}\omega^2\sin(\beta)+2.16\mathrm{mA}\omega^2\cos(\beta)\cos(\alpha)) \quad [4.49]$$

Solving the resultant system of equations leads to:

With the aid of Equations [4.44] through [4.46]

$$F_N = -mA\omega^2(\sin(\beta) + m \times g \qquad [4.50]$$

$$\dot{\mathrm{V}}_{\mathrm{Y}} = \mathrm{A}\omega^2(\cos(\beta)\sin(\alpha-\theta)) - \frac{\mathrm{R_y}}{\mathrm{m}} + \mathrm{V_Z}\,\dot{\theta} \qquad [4.51]$$

$$\dot{\mathrm{V}}_{\mathrm{Z}} = \mathrm{A}\omega^2(\cos(\beta)\cos(\alpha-\theta)) - \frac{\mathrm{R_z}}{\mathrm{m}} - \mathrm{V_y}\,\dot{\theta} \qquad [4.52]$$

From [4.47], and the fact that normal surface reaction will compensate for any rotation about the Y axis:

$$\left|\ddot{\theta}\right| = 0.0037 \times \mathrm{mA}\omega^2\cos(\beta)\sin(\alpha-\theta) \qquad [4.53]$$

The obtained results suggest, as it was with Arc Chute, that the part will always have an angular acceleration $\ddot{\boldsymbol{\theta}}$ around the X axis, which is not desirable for the transportation phenomena, the stability cannot be achieved unless another constraint is imposed.

This condition will hold except for the case where the angles alpha and theta has equal value. In this case $\ddot{\boldsymbol{\theta}} = \mathbf{0}$**,** $\dot{\theta} = 0$ and the part will translate with no rotation.

For this case, the sliding along the Y axis does not occur, the tangential component of the displacement will vanish along with the correspondent friction component. The same conclusions for the sliding conditions on Arc Chute can be reached for this part.

4.4 MAGNET ON BOWL TRACK

In this section, the magnet will be analyzed on the narrow track by reducing the set of forces to a wrench and then equaling the resultant expression to the time rate of change of the angular momentum screw plus the cross product of velocity and momentum screw, in order to get the main parameters governing the transport phenomena. In this case the forces and reactions are affected by the three track angles: one on X-Z plane because the bowl radius, and two on Y-Z, X-Z planes, because the track inclination.

Axes X and Z will be switched to manage those new conditions. By projecting this set of forces over the three axes, taking account on the inclination and vibration angle, the force screw will be:

$$\hat{S}_{F_C} = \begin{bmatrix} R_1\sin(\sigma) - R_2\sin(\sigma) + mA\omega^2\cos(\beta)\cos(\alpha-\theta) - m\times g\sin(\varphi) \\ -R_{1f} - R_{2f} - R_4 \\ \hline R_1\cos(\sigma) + R_2\cos(\sigma) \\ + mA\omega^2\cos(\beta)\sin(\alpha-\theta) + R_3\cos(\delta) - F_N\sin(\delta) \\ \hline + F_N\cos(\delta) + R_3\sin(\delta) - m\times g\cos(\varphi) \\ + mA\omega^2\sin(\beta) \end{bmatrix}$$

$$+\varepsilon \begin{bmatrix} \\ -2.16\times R_3 + 6.79\times\sin(57.12-\delta)\cos(\sigma)(R_1+R_2) \\ \hline -2.16\times R_4 + 6.79\times\sin(57.12-\delta)\sin(\sigma)(R_2-R_1)\cos(\delta) + 3.39\sin(\sigma)(R_2-R_1)\sin(\delta) \\ + (24.55R_1 - 23.85R_2)\cos(\sigma)\sin(\delta) + 3.39(R_{1f}+R_{2f})\sin(\delta) + d\times F_N \\ + mA\omega^2(2.82\sin(\beta)\cos(\delta) + 2.16\cos(\beta)\cos(\alpha-\theta)\cos(\delta) - 2.82\cos(\beta)\sin(\alpha-\theta)\sin(\delta)) \\ \hline - mA\omega^2(2.82\sin(\beta)\sin(\delta) + 2.16\cos(\beta)\cos(\alpha-\theta)\sin(\delta) + 2.82\cos(\beta)\sin(\alpha-\theta)\cos(\delta)) \\ - 6.79\times\sin(57.12-\delta)\sin(\sigma)(R_2-R_1)\sin(\delta) + 3.39\sin(\sigma)(R_2-R_1)\cos(\delta) \\ + (24.55R_1 - 23.85R_2)\cos(\sigma)\cos(\delta) + 3.39(R_{1f}+R_{2f})\cos(\delta) \end{bmatrix}$$

[4.54]

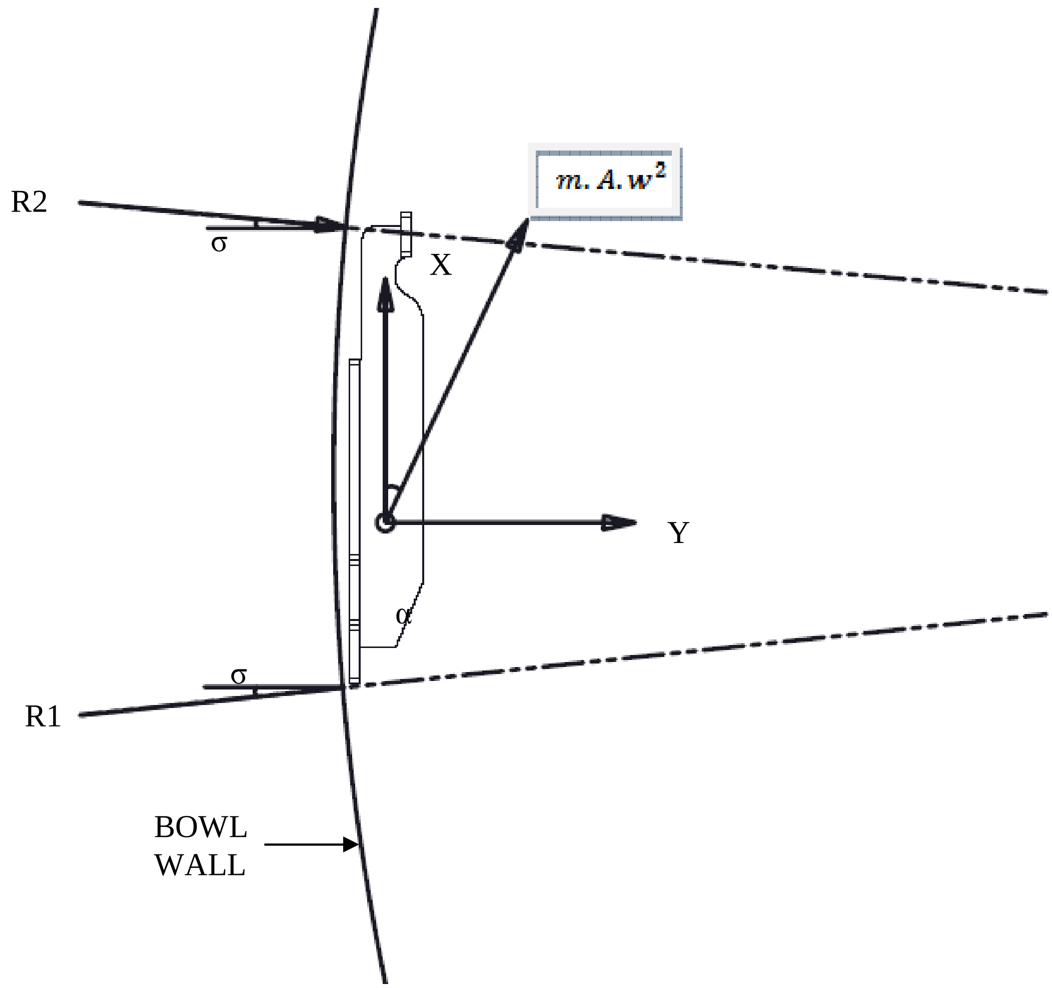

Figure 4-8. Magnet top view on bowl track

Figures 4.9 and 4.10 show the acting forces on the body, including its own weight and vibration force. Forces R_{1f} and R_{2f} (not showed in the drawing) are the friction forces due to the normal reactions R_1 and R_2.

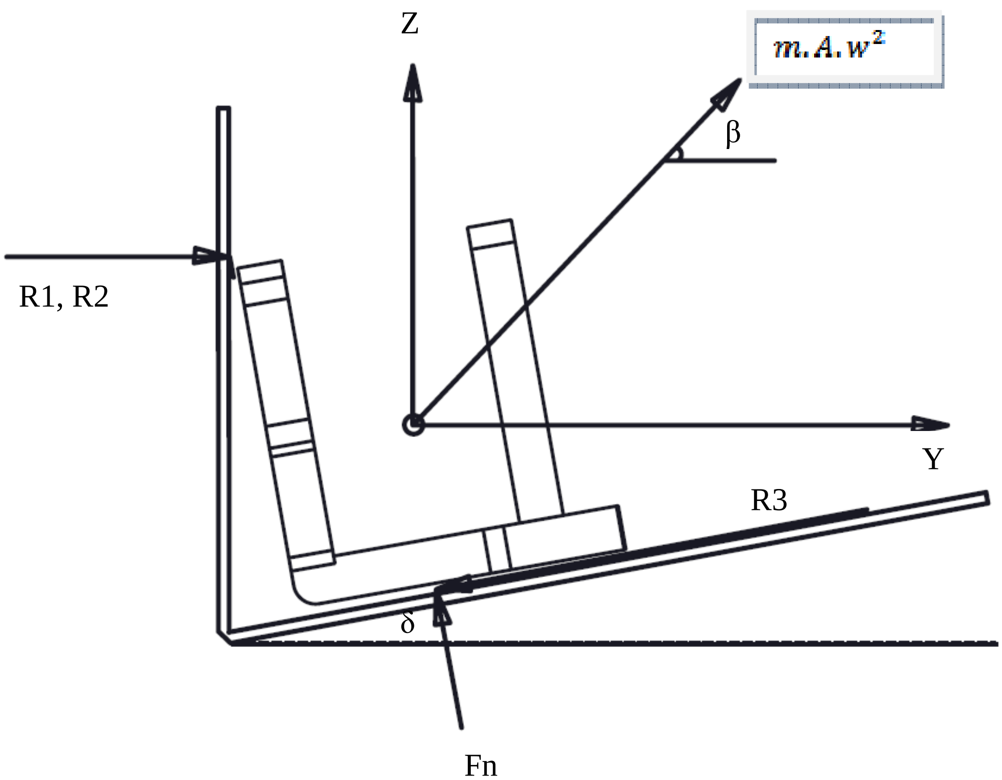

Figure 4-9. Magnet rear view on bowl track

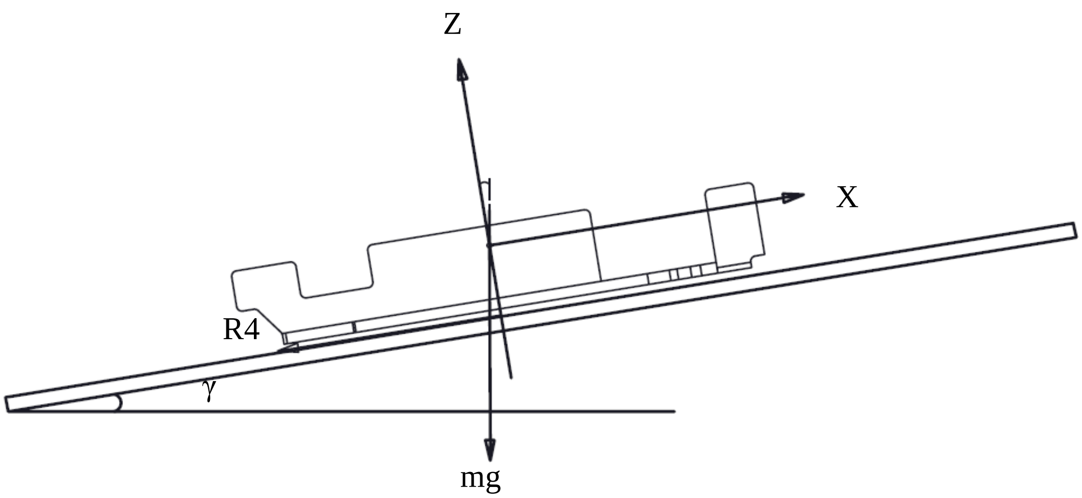

Figure 4-10. Magnet side view on bowl track

Equation [4.54] corresponds to the components of the real and dual parts in the three axes, named X, Y, Z. Then, the axis will be switched, X to Z as related before, equation [4.10] becomes:

$$\frac{d}{dt}\left[\hat{S}_{H_C}\right] = m_C \times \begin{bmatrix} \dot{V}_x \\ \hline \dot{V}_y \\ \hline 0 \end{bmatrix} + \varepsilon \begin{bmatrix} 0 \\ \hline -(I_{YX})\ddot{\theta} \\ \hline -(I_{XX})\ddot{\theta} \end{bmatrix} \qquad [4.55]$$

And [4.12] becomes:

$$\hat{S}_{F_C} = \hat{S}_{P_C} + \frac{d}{dt}\hat{S}_{H_C} = m_C \begin{bmatrix} \dot{V}_X - V_Y\dot{\theta} \\ \hline \dot{V}_y + V_X\dot{\theta} \\ \hline 0 \end{bmatrix} + \varepsilon \begin{bmatrix} (I_{YX})\dot{\theta}^2 \\ \hline -(I_{YX})\ddot{\theta} \\ \hline -(I_{XX})\ddot{\theta} \end{bmatrix}$$

[4.56]

To proceed, the real and dual components are equal to:

REAL PART:

$$\dot{V}_X - V_Y\dot{\theta} = R_1\sin(\sigma) - R_2\sin(\sigma) + mA\omega^2\cos(\beta)\cos(\alpha-\theta) - m\times g\sin(\varphi) \qquad [4.57]$$
$$-R_{1f} - R_{2f} - R_4$$

$$\dot{V}_y + V_X\dot{\theta} = R_1\cos(\sigma) + R_2\cos(\sigma) + mA\omega^2\cos(\beta)\sin(\alpha-\theta)$$
$$+R_3\cos(\delta) - F_N\sin(\delta)$$

[4.58]

$$0 = F_N\cos(\delta) + R_3\sin(\delta) - m\times g\cos(\varphi)$$
$$+mA\omega^2\sin(\beta) \qquad [4.59]$$

DUAL PART:

$$-10.91\dot{\theta}^2 = -2.16\times R_3 + 6.79\times\sin(57.12-\delta)\cos(\sigma)(R_1+R_2) \qquad [4.60]$$

$$\begin{aligned}10.91\times\ddot{\theta} &= -2.16\times R_4 + 6.79\times\sin(57.12-\delta)\sin(\sigma)(R_2-R_1)\cos(\delta)\\ &+3.39\sin(\sigma)(R_2-R_1)\sin(\delta)+(24.55R_1-23.85R_2)\cos(\sigma)\sin(\delta)\\ &+3.39(R_{1f}+R_{2f})\sin(\delta)+d\times F_N + mA\omega^2(2.82\sin(\beta)\cos(\delta)\\ &+2.16\cos(\beta)\cos(\alpha-\theta)\cos(\delta)-2.82\cos(\beta)\sin(\alpha-\theta)\sin(\delta))\end{aligned} \qquad [4.61]$$

$$\begin{aligned}-755.91\ddot{\theta} &= -mA\omega^2(2.82\sin(\beta)\sin(\delta)+2.16\cos(\beta)\cos(\alpha-\theta)\sin(\delta)\\ &+2.82\cos(\beta)\sin(\alpha-\theta)\cos(\delta))-6.79\times\sin(57.12-\delta)\sin(\sigma)(R_2-R_1)\sin(\delta)\\ &+3.39\sin(\sigma)(R_2-R_1)\cos(\delta)+(24.55R_1-23.85R_2)\cos(\sigma)\cos(\delta)\\ &+3.39(R_{1f}+R_{2f})\cos(\delta)\end{aligned} \qquad [4.62]$$

The bowl wall constrains rotation about the Z axis (we assume that the part and bowl wall keep in contact at all times), having

$$\dot{\theta} = 0$$

$$\ddot{\theta} = 0$$

The obtained results suggests that if the angle δ is equal to 57.12 the reaction R_3 will be zero, so there would not be displacement in the Y (radial) direction. This condition is expected for a forward conveying.

In this case the bowl wall prevents the rotation around the Z axis, which is a desirable stability condition for the part.

4.5 SUMMARY

In this chapter the Screw Theory was applied to develop equations that describe the state of motion of the parts arc chute and magnet. The results for the part Arc Chute on the bowl floor will be modeled on chapter 5 for typical bowl parameters for a part displacing independent of its shape inside a bowl feeder, assumed to move bodily with simple harmonic motion; the air resistance is neglected (Boothroyd et al., 1992, Diaz, 2004).

5 SIMULATION RESULTS

In this analysis the motion parameters such as frequency (f), vibration amplitude (A_0), friction coefficient (μ) and excitation angles α and β (alpha and beta) will be plotted to analyze the motion of the part Arc Chute on the bowl floor. These motion parameters are chosen for typical values.

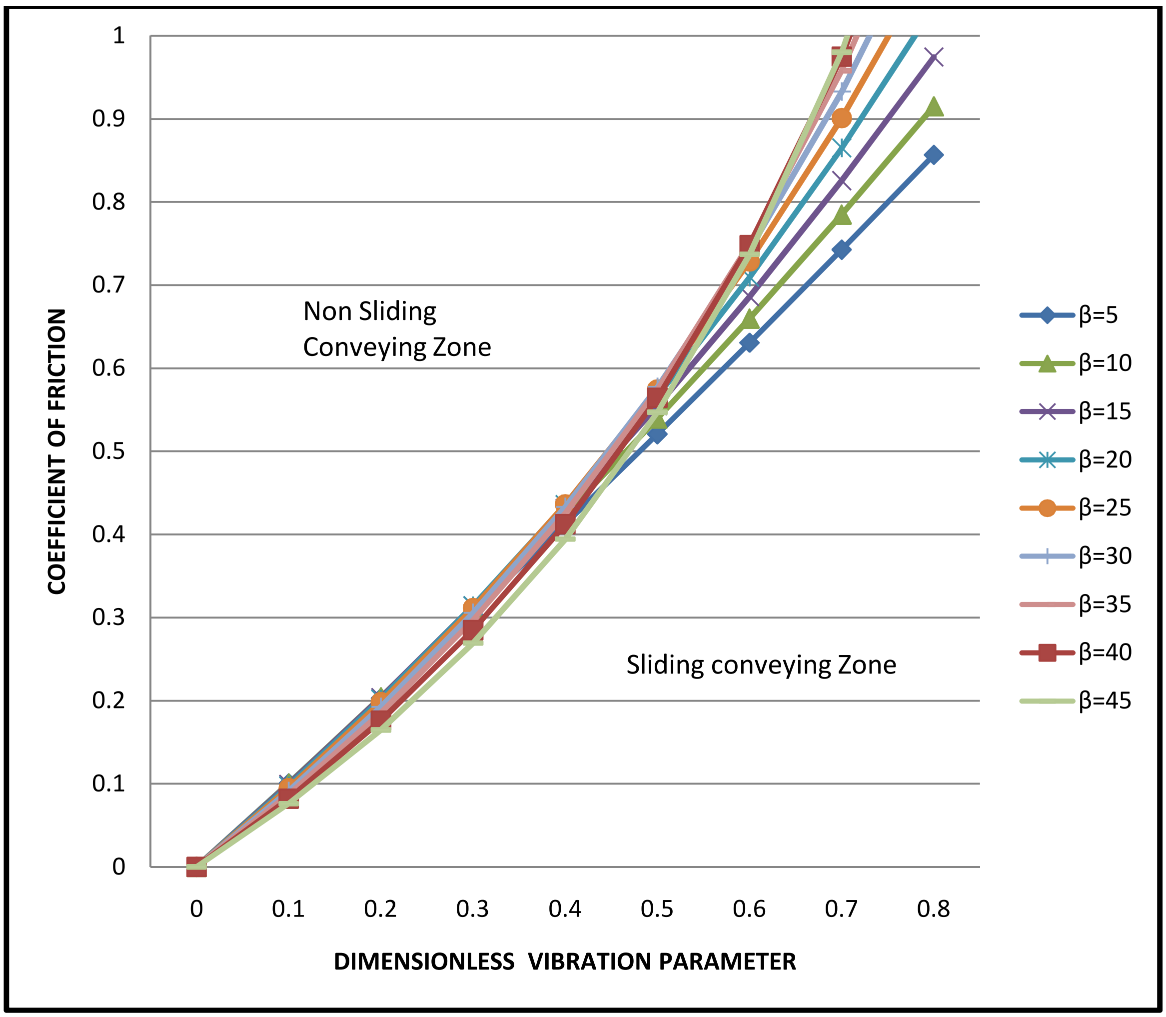

Figure 5-1.Limiting Condition for sliding along the Z axis.

Figure 5-1 is a plot of equation [4.28]; it shows the limiting sliding condition for different values of angle β, and the case where the angles α and θ have the same value. The sliding is not desired in the feeding process, because it represents a vibration energy loss and, consequently, the transportation velocity is reduced (Diaz, 2004). It can be seen that the sliding region will be increased for large β angles.

Figures 5-2 through 5-4 are plots of equation [4.27] for different values of angle β; Figure 5-5 is a contour line of Figure 5-2. Those graphs show the effect of angles: α and θ and the dimensionless vibration parameter (vibration amplitude plus the square of the angular frequency divided by gravity acceleration). The zone under the surface is the sliding area.

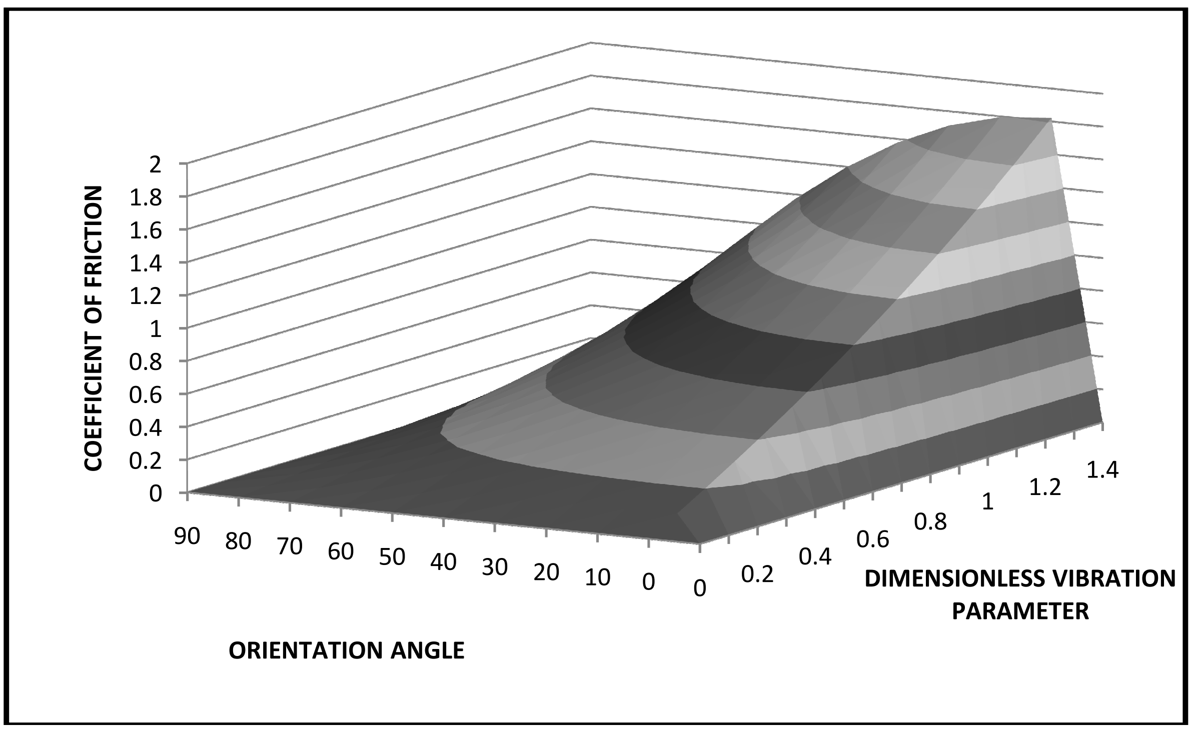

Figure 5-2.Contour surface for the friction coefficient. Angle β=10°

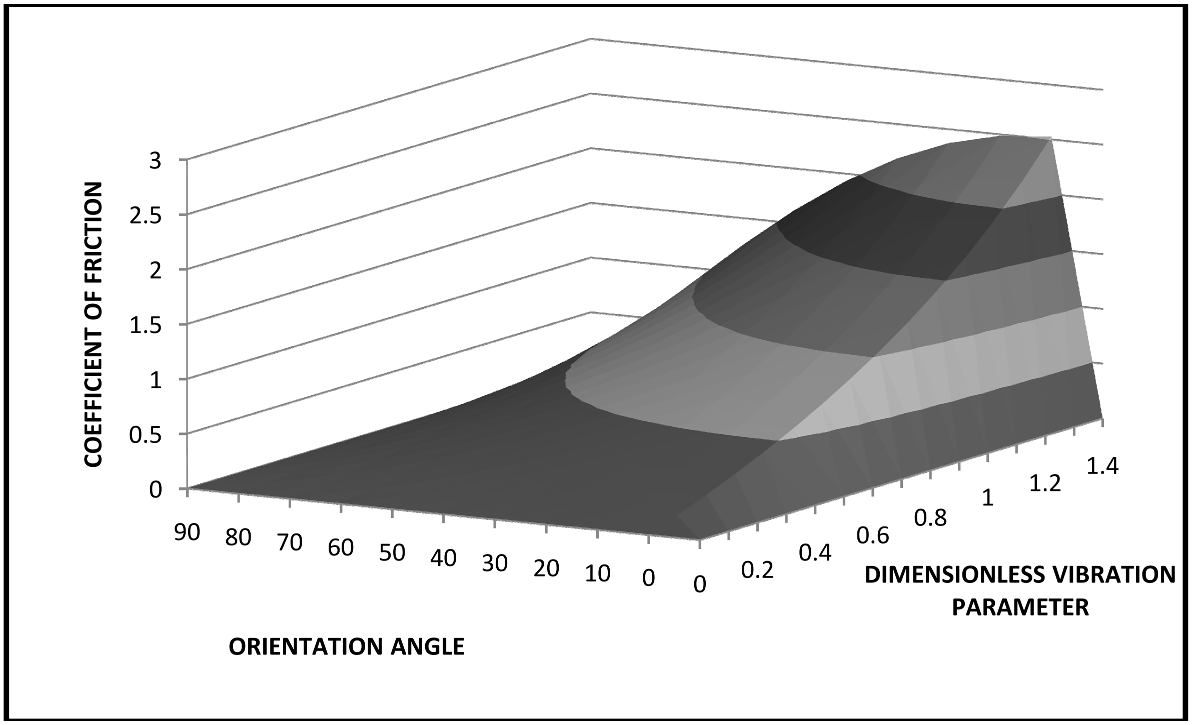

Figure 5-3.Contour surface for the friction coefficient. Angle β=20°

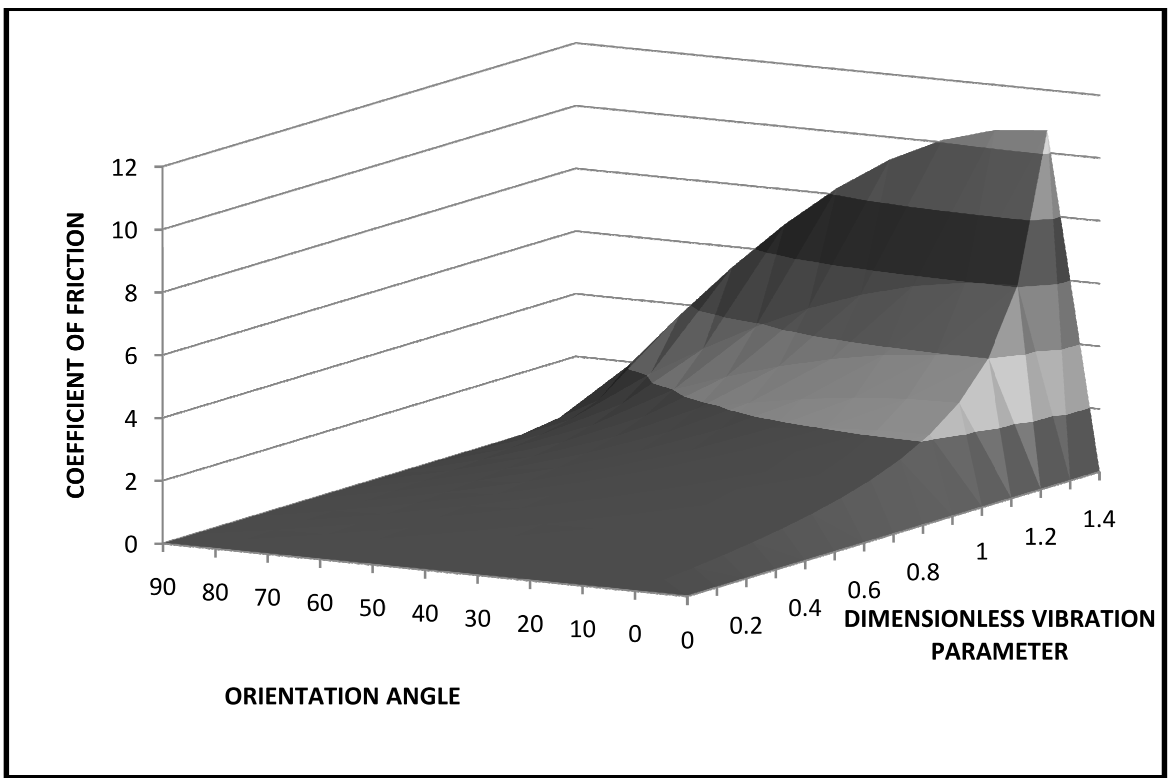

Figure 5-4.Contour surface for the friction coefficient Angle. β=40°

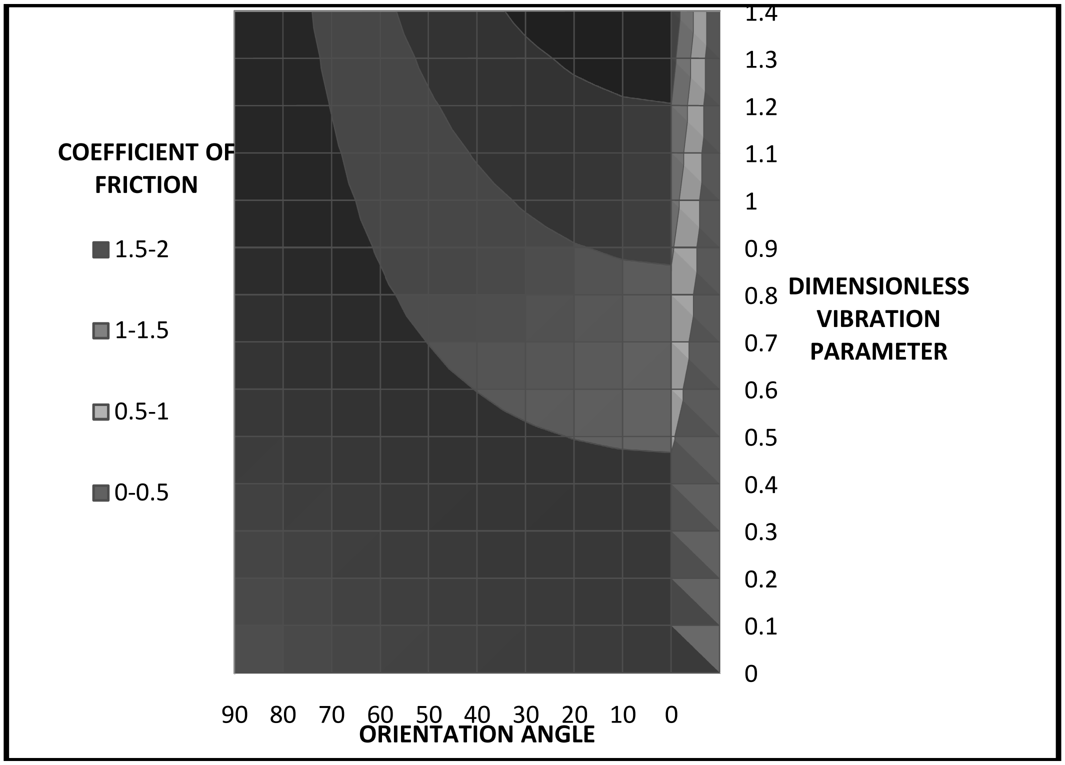

Figure 5-5. Contour lines for the friction coefficient.β=10°

The Figure 5.6 shows the acceleration in the z´ direction, as defined in Figure 4-1 for Arc Chute on bowl floor. The used values for the parameters were: f=60 Hz, Ao =0.0005m, g=9.8m/s^2. It can be seen that there is a maximum acceleration for values of angle β between 40 and 60 degrees, and high values of coefficient of friction. Consequently in this region the transportation velocity will be maximized.

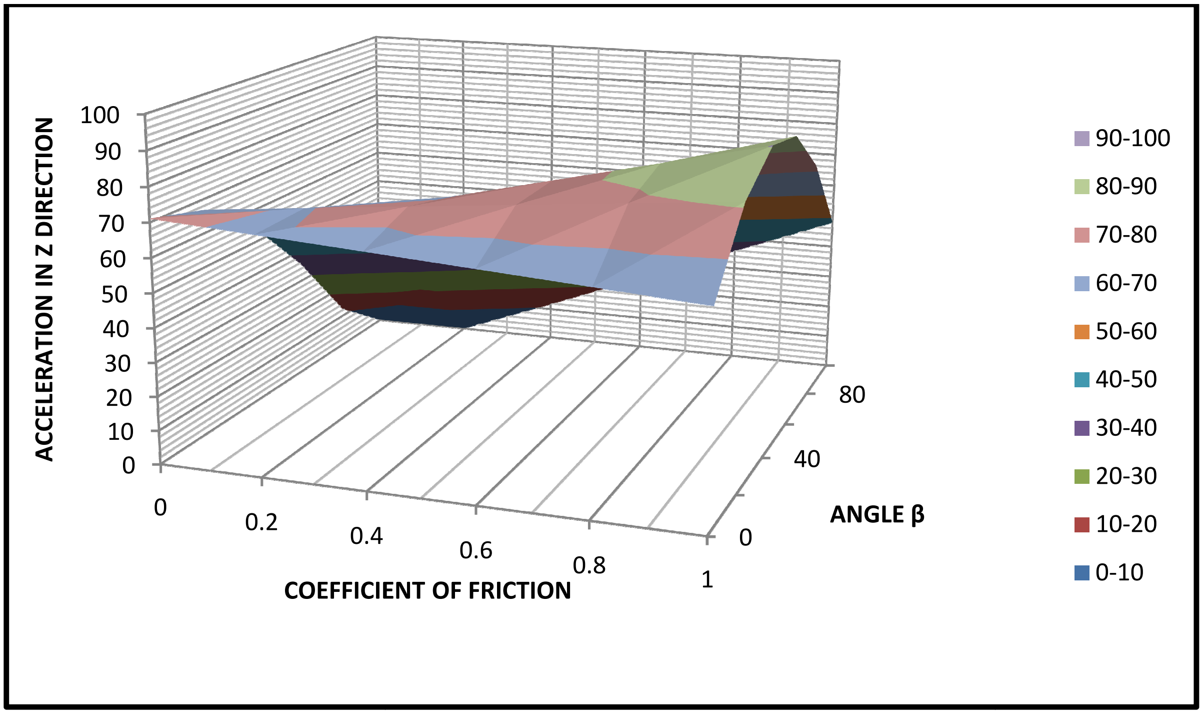

Figure 5-6. Acceleration in direction Z against β and μ.

The Figure 5.7 shows the acceleration in the z direction, plotted against the amplitude of vibration and the frequency for part Arc Chute on the bowl floor. The used values for the parameters were: β=20, g=9.8m/s^2 and μ=0.5. It can be seen that the acceleration is higher for higher values of amplitude of vibration as it is expected, and so the transportation velocity. However the frequency effect is not necessary to increase the transportation velocity taking account on the effect of hoping for vibratory bowl feeders, where the parts hop in the bowl with low velocity or no velocity at all.

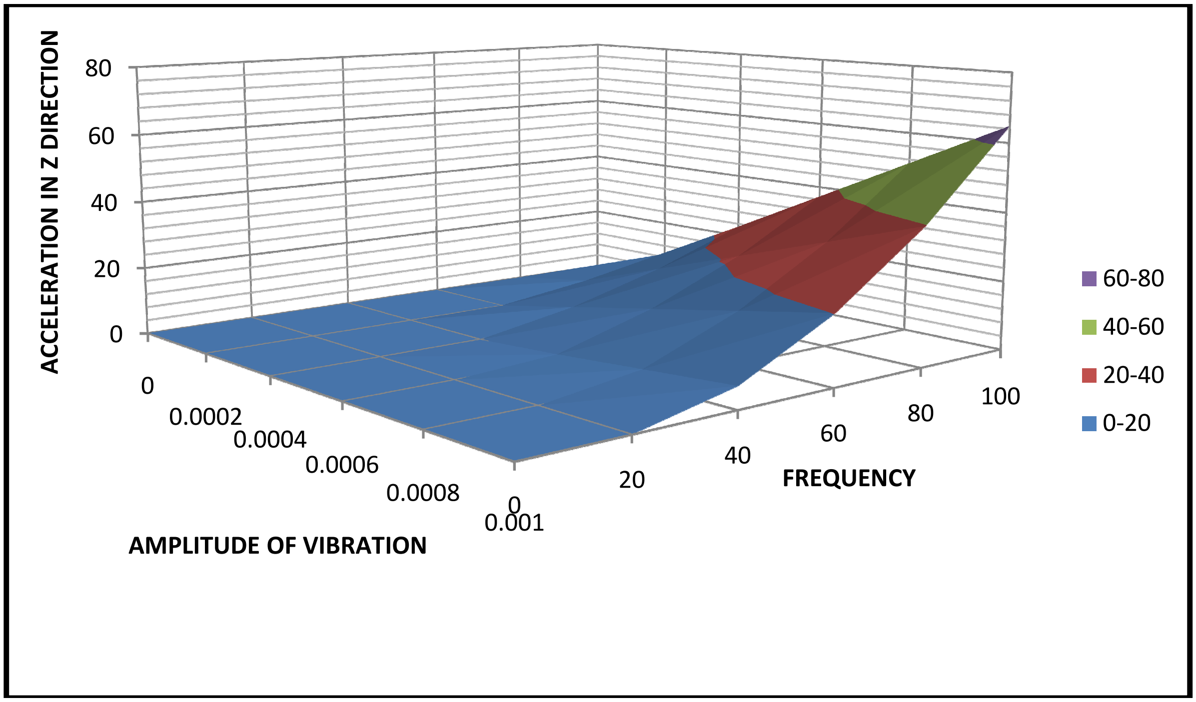

Figure 5-7. Acceleration in direction Z against f and Ao.

6 CONCLUSIONS AND RECOMEDATIONS

6.1 CONLUSIONS

1. The natural resting probability profiles of parts inside vibratory bowl feeders can be analyzed taking into account only geometric parameters, which reduce a considerable amount of work for the feeders design.
2. The PMI method shows good probability predictions for various aspects of the parts Arc Chute and "T" shape part, when compared with CSA, which is widely documented as an analytical method.
3. The PMI method was not satisfactory to analyze the natural resting aspect probability profile of "T" shape part when compared with experimental data.
4. The advantage of the PMI method is the easy implementation and calculation for very complex geometries.
5. The Newton-Euler equation proved to be a valuable tool in the analysis of rigid body dynamics with complex restrictions. Based on that equation the relationships between the main parameters governing the transport phenomena: amplitude and frequency of vibration, coefficient of friction and excitation angles where disclosed.

6. In the case of motion of selected parts on the bowl floor and equal values for angles α and θ, increasing angle β will have the effect of reducing the size of the non sliding conveying zone.
7. Figure 5.6 shows high acceleration values for the part with high values of coefficient of friction and angle β in the range of 40° to 60°.
8. For different combination of angles α and θ, equation [4.27] provides the required conditions of the friction coefficient and dimensionless vibration parameter in order to achieve non sliding conveying.

6.2 RECOMENDATIONS

For the future work it is recommended to test more parts in order to better check the accuracy of the PMI method. In addition, the number of tests and the amount of experimental data used could be increased in order to have a better drop test probability profile.

It is also recommended to study the effect of product of inertia into the PMI method for complex geometries.

In the case of the dynamics of parts, the analysis via Screw Theory can be improved including systems of screws for multibody cases.

7 BIBLIOGRAPHY

[1] Ball, R. S., 1900, "A Treatise on the Theory of Screws", Cambridge University Press

[2] Boothroyd, Geoffrey. 1992, "Assembly Automation and Product Design", Marcel Dekker Inc.

[3] Davidson, J.K. and Hunt, K.H. 2003, "Robots and Screw Theory", Oxford Press.

[4] Díaz, James. 2004. "Dynamics of Parts on Narrow Tracks Using the Multibody Theory". Thesis M.S. University of Puerto Rico, Mayagüez, P.R.

[5] Lamb, D. 2003, "Treatise on the Theory of Screws", Internet reference.

[6] Lipkin, H. and Duffy, J. 2002, "Sir Robert Stawell Ball and Methodologies of Modern Screw Theory", Journal of Mechanical Engineering Science.

[7] Ngoi, B.K.A., Lee, S.S.G., Lim, L.E.N. 1995a, "Analyzing the Natural Resting Aspects of a Component by its Centroid Solid Angle", Journal of Electronic Manufacturing, Vol. 53 No 3, pp. 193-197.

[8] Ngoi, B.K.A., Lee, S.S.G., Lim, L.E.N. 1995b, "Analyzing the Probabilities of the Natural Resting Aspects of a Component with a Displaced Center of Gravity", International Journal of Production Research, Vol. 33 No 9, pp. 2387-2394.

[9] Ngoi, B.K.A., Lee, S.S.G., Lim, L.E.N., Lye, S.W. 1995c. "Analyzing the Natural Resting Aspects of a Component for Automated Assembly". Journal of Engineering Manufacture, Vol. 209, pp. 125-135.

[10] Ngoi, B.K.A., Lee, S.S.G., Lim, L.E.N. 1995d, "Analyzing the Natural Resting Aspects of a complex Part", International Journal of Production Research, Vol. 33 No 11, pp. 3163-3172.

[11] Ngoi, B.K.A., Lye, S.W, Chen, J. 1997, "Analyzing the Natural Resting Aspects of a complex shaped Part on a hard surface for automated parts feeding", Proceedings of the Institution of Mechanical Engineers; 1997;211,6;Pro Quest Science Journals. pp 435-442.

[12] Pennock, Gordon R. and Meehan, Patrick J. 2002. "Geometric Insight into the Dynamics of a Rigid Body Using the Spatial Triangle of Screw". Journal of Mechanical Design, vol 124: pp 684-689.

[13] Pennock, Gordon R. and Oncu B.A. 1992. "Application of Screw Theory to Rigid Body Dynamics". Journal of Mechanical Design, ASME vol 114: pp 263-269.

[14] Pennock, Gordon R. 1992. "An extension of Screw Theory to the dynamics of a two-cylindric Robot Manipulator". Journal of Mechanical Design, ASME

[15] Rincón, Amílcar. 2002. "Estudio del Comportamiento de Piezas Complejas en un Alimentador Vibratorio" Thesis M.S. University of Puerto Rico, Mayagüez, P.R.

[16] Santos, Abigail. 2004. "Analyzing the Parts Behavior in a Vibratory Bowl Feeder to Predict the Dynamic Probability Profile". Thesis M.S. University of Puerto Rico, Mayagüez, P.R

[17] Wang J., Huang C., 2003. "The finite Screw System Associated with the Displacement of a Line" Journal of Mechanical Design", ASME Vol. 125 pp105-109.